

APPLICATIONS OF A PLUME MODEL
TO
PHOTOGRAPHICALLY OBSERVED CONVECTION

by

PATRICIA ANN BUDER


B.S., Saint Louis University
1971

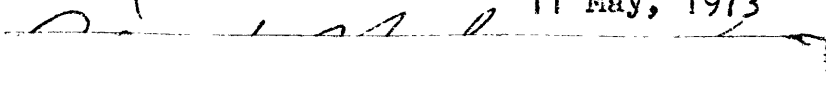
SUBMITTED IN PARTIAL FULFILLMENT
OF THE REQUIREMENTS FOR THE
DEGREE OF MASTER OF
SCIENCE

at the

MASSACHUSETTS INSTITUTE OF
TECHNOLOGY

May, 1973

Signature of Author 
Department of Meteorology
11 May, 1973

Certified by 
Thesis Supervisor

Accepted by
Chairman, Departmental Committee
on Graduate Students

AbstractAPPLICATIONS OF A PLUME MODEL TO PHOTOGRAPHICALLY OBSERVED
CONVECTION

by

Patricia Ann Buder

Submitted to the Department of Meteorology on 11 May, 1973 in partial fulfillment of the requirements for the degree of Master of Science.

A steady-state entraining plume model was used to predict cumulus convection, and the results were compared to photogrammetrically observed clouds. The data utilized in this thesis was recorded during operation of Cloud Puff IV, a field experiment undertaken in 1969 in southern New Mexico over the Organ Mountain range. It was noted that the plume model was sensitive to a number of factors, each of which was investigated. Cloud calculations were found to vary substantially according to the choice of cloud base level, initial radius and vertical velocity at cloud base and location of radiosonde sounding input levels. Little sensitivity was shown to the humidity profile above the level at which dewpoint information ceased to be available. Measured cloud base heights seemed to increase slightly with time on each of the three test days. Variability of bases at a given time was of the order of one thousand feet or less. Error in photogrammetric measurements was sufficient to produce this variability, but it is entirely reasonable that such differences exist over mountainous terrain. Cloud base heights were quite close to the convective condensation level of the morning sounding on each day and were below both the lifting and convective condensation levels of the afternoon soundings. Variability of cloud top heights corresponded closely with model predictions from three sets of initial radii and vertical velocities for each day's medium and large sized clouds. The model was unable to predict with realistic vertical size profiles and vertical velocity profiles the heights of cloud tops for the smaller clouds that were observed. However, an assumption in the model formulation was that the cloud was steady-state and in the mature stage of development, while the observed small clouds were in an initial stage of development.

Thesis Supervisor: Edward N. Lorenz
Title: Professor of Meteorology

Table of Contents

	<u>Page</u>
1. Introduction	4
2. Survey of similar investigations	5
3. Description of the plume model	9
4. Description of the data	12
5. Results of investigation of model sensitivity	14
Sensitivity to choice of cloud base height	14
Sensitivity to choice of sounding levels	17
Sensitivity to choice of initial radius and vertical velocity	21
Sensitivity to humidity profile	24
6. Model predictions compared with observed growth	26
Description of photogrammetric technique	26
Comparison of predicted and measured cloud base heights	29
Comparison of predicted and measured cloud top heights	31
7. Conclusions and Recommendations	33
List of Tables and Figures	37
Acknowledgments	86
References	87

1. Introduction

It was desired to make a study of cumulus cloud development over mountainous terrain, using a numerical convection model to predict development and comparing the computed clouds with observations of the convection that actually occurred.

Cloud Puff IV, a field experiment undertaken in 1969 near the Organ Mountains in southern New Mexico, included photographic data from stereo cameras suitable for photogrammetric measurements. The data from this project was chosen for use in this investigation because of the availability of these photographs, frequent radiosonde soundings and other useful information.

With the radiosonde soundings, the plume model written at MIT by Professor Norman Phillips was used to predict the development of convection and the results compared to the dimensions obtained from the photogrammetric measurements. It was found necessary to investigate the sensitivities of the numerical model to initial data input in order to gauge the validity of any results.

The answers to several questions were sought from the predicted and measured results. The numerical model did not account in any way for topographic variation. The question arose of whether the photographically observed cloud bases were at the sounding's lifting condensation level, the convective condensation level or somewhere in between and if this could be attributed to lifting by the

mountains, an elevated heat source, or both. Over flat terrain it is known that cloud bases form at a more or less constant height. Is this true over mountains, or is there a large variance in the height at which bases form? Another consideration was whether the variability of predicted cloud tops was comparable to the variability of the cloud tops in the real atmosphere. Perhaps atmospheric conditions vary substantially from one location to another and the clouds that form vary considerably also. Or will a very slight horizontal variation in atmospheric conditions, only a few tenths of a degree in temperature and dewpoint, produce quite different clouds? It is considerations such as these that are to be investigated in this thesis.

2. Survey of investigations using numerical convection models

Several numerical models of cumulus convection have been formulated, and some of the more well known of these will be discussed. The models generally fall into two classes.

One approach is to set up the complete hydrodynamic equations in finite difference form and allow a computer to solve them in a series of finite time steps, beginning with a prescribed initial condition. This type of model is called a "field of motion" model.

An early such model was described by Malkus and Witt (1959). In this dry model, two-dimensional motions in ver-

tical planes were considered, and a lower unstable or neutral layer was topped by a more stable one. Initially a potential temperature perturbation was introduced and finite difference forms of equations governing vorticity, temperature and motion fields were solved in a series of time steps. The calculations had to be terminated after a period corresponding to five to seven minutes due to the growth of numerical errors.

Since that time more complicated geometries, the simulation of condensation of water vapor into liquid, the transport of liquid and water vapor and even the effects of the ice phase have been introduced to "field of motion" models. However, such models have been forced to parameterize the non-linear processes governing particle growth, since condensation, coalescence, freezing, crystal growth, etc., are analytically intractable processes.

F.W. Murray (1970) has succeeded in modeling the growth and fallout of liquid precipitation. His model is based on the Boussinesq approximation which permits the derivation of a vorticity equation locally and from this the stream function is found.

Simpson, Wiggert and others from the Experimental Meteorology Laboratory have used numerical models operationally to predict effects of seeding. Simpson and Wiggert (1971) used an existing cumulus model and altered it to simulate the dynamic effects of seeding. Wiggert (1972) describes modifications made at EML to Murray's

model. Changes in the advection scheme were made and Kessler's precipitation parameterization scheme was substituted for the non-fallout of liquid water treatment. The initial perturbation and the observed cumulus tower diameter and cloud base height were presumed to be related. Also, the lower levels of soundings taken over land were restructured to better emulate ambient conditions when clouds grew over the sea.

Another "field of motion" model is that of Gray and Lopez (1972). It is basically one-dimensional and parametric. The turbulent and microphysical phenomena are expressed in terms of cloud-scale variables, while the dynamical and thermodynamical processes are treated in a prognostic fashion. In order to avoid the common similarity assumption, mixing between cloud and environment is parameterized in terms of the turbulence intensity of the interior and exterior of the cloud.

The model of Weinstein (1970) is one-dimensional and time dependent. It considers the processes of horizontal mixing, evaporation, precipitation generation and freezing as well as the dynamic and thermodynamic processes of cumuli. A slightly modified version of this model was used operationally in Cloud Puff III, a field experiment conducted at White Sands, New Mexico, to determine the predicted height of unseeded cumulus tops, the increment of height which would result from seeding and threshold values of various cloud parameters.

The second type of dynamic model has been called an "entity" model. In these a cumulus cloud is likened to an entity, such as a plume or jet, or a bubble. Major simplifications result from this likeness. The number of differential equations is reduced, and semi-empirical laws can be derived from theories or measurements of the entity. This allows complete specification of every parameter in the equations except for properties to be predicted.

The Squires and Turner (1962) model and Scorer's bubble theory are of the "entity" type. The plume model used in this thesis is a modified version of the Squires and Turner model; its properties are discussed under Description of the plume model.

While the "field of motion" type of model seems to suggest a more thorough formulation with an explicit cloud physics treatment, there are serious limitations to its use, some of which apply also to "entity" models. For example, the results are quite sensitive to the form of the initial perturbation and to the form of expression of the equations in relation to a finite difference grid. It is not at all clear that the present representations of entrainment are completely correct. The "entity" models avoid some of the pitfalls of other models, but they introduce assumptions of their own. Nevertheless, a plume model was chosen for use in this thesis and its sensitivities were examined.

3. Description of the plume model

This study uses a computer model to predict cumulus cloud development that is based on a steady-state, condensing plume which entrains environmental air by assuming that the inflow velocity at any height is proportional to the upward velocity of the plume. It is a slight modification of one described by Squires and Turner (1962) and was formulated by Professor Norman A. Phillips of the Massachusetts Institute of Technology and programmed by Tony Hollingsworth.

The model uses an entropy procedure to account for heat carried by condensed water; it ignores precipitation and assumes the environment has no condensed water. The shape of the cloud and its other properties follow from the dynamics, and cloud development is size-dependent.

A top-hat profile in combination with the Morton, Taylor and Turner entrainment hypothesis can be used to express conservation of mass, momentum, water substance and entropy in the saturated plume.

$$\frac{d}{dz} (b^2 w \rho_c) = 2 \alpha_e b w \rho_c$$

$$\frac{d}{dz} (b^2 w^2 \rho_c) = g b^2 (\rho_c - \rho)$$

$$\frac{d}{dz} (b^2 w \rho_c r) = 2 \alpha_e b w \rho_c r_c$$

$$\frac{d}{dz} (b^2 w \rho_c \lambda) = 2 \alpha_e b w \rho_c \lambda_c$$

where ρ = plume density
 λ = water mixing ratio (vapor + liquid or solid)
 s = specific entropy
 b = plume radius
 w = plume vertical velocity

and the subscript e refers to the environment.

α_e , the entrainment factor, was taken as 0.1, as was indicated by the laboratory work of Morton and Turner.

Define

$$\begin{aligned} dp &= -\rho_e g dz \\ u &= b^2 w \rho_e \\ v &= b^2 w \sqrt{\rho_e} \\ h &= b^2 w \rho_e \lambda = u \lambda \\ \sigma &= b^2 w \rho_e S = u S \\ S &= \frac{s}{R_d} \end{aligned}$$

$$Z = -\ln(P/P_{00}) = -\ln P$$

$$D = \frac{2 dz}{g} \frac{p}{\sqrt{\rho_e}}$$

The equations then become

$$\frac{du}{dZ} = Dv$$

$$\frac{dv}{dZ} = \frac{1}{2} \frac{P_{00} P}{\rho_e} \left(1 - \frac{p}{\rho_e}\right) \frac{u^2}{v^3}$$

$$\frac{dh}{dZ} = \lambda_e (D\sigma)$$

$$\frac{d\sigma}{dz} = \sum_e (Dv)$$

$$\rho = \rho(r, P, S)$$

The integration of these five equations is done by a Runge-Kutta procedure within each of the successive layers defined by radiosonde data. The expressions on the left side of this system are treated as unknowns, to which values must be assigned at cloud base. Squires and Turner assume that the virtual temperature excess at cloud base is zero, since it seems that thunderstorm updrafts derive most of their energy from the latent heats of condensation and freezing rather than from surface heat sources, and once triggered merely release the energy stored in the environment. Essentially, it is assumed that at cloud base the specific entropy of the plume equals that of the environment and the plume mixing ratio equals the environmental mixing ratio. Thus, the plume is initiated by an updraft at its base, with assigned values of vertical velocity and radius, rather than by excess buoyancy at cloud base.

With the proper initial conditions somewhat realistic clouds can be simulated. However, the plume model contains several serious inadequacies. The specification of the initial conditions is arbitrary and the evolutionary process of cloud growth is ignored. Lateral growth, the development of downdrafts and drag from falling precipitation undoubtedly have a marked effect on cloud

dynamics. The above described treatment is restricted to the case of no general wind shear. In mid-latitude convection strong shear is often present, and the assumption of a vertical plume in a non-turbulent environment is not valid. When the environment is turbulent to a degree comparable with the updraft an exchange of mass in both directions would necessitate the introduction of detrainment as well as entrainment. It appears that a more realistic arrangement would consist of updrafts and downdrafts, side by side, tilted in the vertical and including a mass flux in both directions.

4. Description of the data

The data used for this study were collected during operation of Cloud Puff IV, a joint Air Force-Navy-Army field experiment in weather modification, and were obtained from Air Force Cambridge Research Laboratories, Bedford, Massachusetts. The principal participants were the Earth and Planetary Sciences Division of the Naval Weapons Center, the Cloud Physics Branch of AFCRL and the Atmospheric Physics Division of White Sands Missile Range. Cloud Puff IV was conducted near Las Cruces, New Mexico at the White Sands Missile Range, over and near the Organ Mountains.

Of the numerous types of data recorded during this project, in this thesis use was made predominantly of radiosonde soundings and ground based stereo photographs.

Figure 1 illustrates the location of the equipment in relation to the mountain range. The data include transcripts of aircraft crew dialogue recorded during operational flights over the test area. Occasionally these transcripts provided information on cloud base and top heights. Cloud development was located in relation to topographic features through mosaic strips assembled from U-2 photographs which were taken from a height of approximately 66,000 feet MSL.

Radiosonde soundings were made at frequent intervals and those used herein were released from White Sands. Data points were at 500 foot intervals from the surface to approximately 70,000 feet MSL and higher.

During the three days of operation cited in this study, 15 July 69, 22 July 69 and 25 July 69, vertical wind shear was observed at all sounding times. On the 15th surface winds were southerly with upper level winds generally from the southeast. Hence, the sounding was upwind of the mountains, with convection developing over the range and moving generally westward. The other two days exhibited northwesterly surface winds and considerable vertical shear; in these cases it is observed that the soundings were not upwind of the peaks.

Morning and afternoon soundings were used in the plume model for each of the three test days. The six soundings tested are shown in Figures 2 through 4. On 15 July 69 and 25 July 69 the 0500 Mountain Standard Time and the 1300 MST radiosondes were used. On 22 July 69 the soundings

were from 0700 MST and 1300 MST.

Cloud base and top measurements were made using photographs from the ground based T-11 stereo cameras located near Las Cruces. These cameras were operated during the period each day from the beginning of cloud formation until one hour following termination of the project's final test case, photographs being taken every few minutes. The location of cloud elements in the vertical was accomplished through photogrammetric techniques in a manner similar to that described by Glass and Carlson (1963). The photogrammetric methods employed in this thesis are subsequently discussed in detail.

5. Results of investigation of model sensitivity

One of the problems encountered with the plume model is its sensitivity to the input data, e.g., cloud base height, radius and vertical velocity at cloud base, choice of sounding levels, etc. In order to predict cloud development with such a model, it was deemed necessary to investigate the effects of such initial specifications on the model's prediction capabilities. Each class of input data was varied over a considerable range. The results were analyzed in an attempt to find physically reasonable limits on the choice of each parameter that must be initially specified.

Sensitivity to choice of cloud base height

Since the clouds formed over mountains it was unclear what level would be an appropriate choice for cloud base.

Two different methods were employed to select a base height from radiosonde soundings. For a range of initial radii and vertical velocities several runs of the model were made using as cloud base both the lifting condensation level and the convective condensation level. Figures 5 through 10 are samples of the graphs used to compile Table 1. These vertical profiles illustrate the differences in cloud growth. In all cases except one the use of the LCL as cloud base level allowed clouds to become more fully developed, in vertical extent and updraft velocity, than the use of the CCL. This was considerably more pronounced for morning soundings, which had 100 mb to 150 mb differences between the LCL and the CCL, than for the afternoon soundings, where there were only 10 mb to 20 mb differences. This is reasonable, as more moisture is contained in a vertical column originating at low levels than in one with cloud base at a higher level; in addition, a smaller dew-point depression generally exists at lower levels than at higher levels. Since the growth of the plume is dependent for the most part on the latent heats of condensation and freezing, the more moisture available, the greater the development of the cloud, given a relatively unstable sounding.

Four combinations of initial radii and vertical velocities, 1000 meters and 1 meter per second, 2000 m and 1 mps, 1000 m and 2 mps, and 2000 m and 2 mps, were used to test the differences in growth between clouds with a base at the

LCL and those with bases at the CCL. Table 1 lists these differences for the six soundings investigated. For 15 July 69 at 0500 MST the differences ranged from 7100 feet to 11,800 feet. The 0500 MST sounding shows considerable low level moisture to be gained by using the LCL of 825 mb rather than the CCL of 664 mb. The 1300 MST sounding of the same day had an LCL of 666 mb, only 10 mb lower than its CCL of 656 mb. The differences in cloud tops were 700 feet to 2400 feet, considerably less than when the LCL and CCL are more widely separated in height. These figures accentuate the dependency of cloud growth on the base level chosen; a difference of only 10 mb in cloud base can result in cloud top differences of thousands of feet. However, it is not at all clear that this is a product of the plume model and is not the case in the real atmosphere.

The morning sounding for 22 July 69 showed an LCL of 850 mb and a CCL of 760 mb, with cloud top differences ranging from 1500 feet to 5200 feet. Large differences were again encountered with the 0500 MST sounding on 25 July 69, with an LCL of 783 mb and a CCL of 688 mb. The range was 3400 feet to 19,800 feet. These differences lend support to the idea that the model is quite sensitive to the level chosen as cloud base.

The anomalous case, 1300 MST on 22 July 69, exhibited higher tops using the CCL as cloud base than using the LCL for all initial conditions tested. The LCL was 680 mb

and the CCL was 654 mb. Figure 11 illustrates the sounding as the computer interprets it; it is apparent that the computer interpretation of the sounding is dependent on the pressure levels that are input. The model interpolates between data input levels, and it is seen that the moisture content of the plume is greatly enhanced in the case of the CCL cloud base as a result of the interpolation procedure. Because of the necessary saturation at cloud base, interpolation between the initial data point and the next input level produced greater moisture content in the lowest layer than the model interpreted for the same layer in the case with the LCL as cloud base. Therefore, the higher tops observed in this case are not physically realistic, but rather are a product of a particular choice of sounding input levels and the computer interpolation procedure.

Sensitivity to choice of sounding levels

As was noted in the previous section, the model predictions are quite sensitive to the pressure levels chosen as data input levels. The model is capable of accommodating up to twenty levels. Initially the assumption was made that significant levels distributed approximately evenly with height would be appropriate, and predictions were made with such data levels. However, the possibility presented itself that the use of more lower levels in place of the several levels included above 100 mb, while retaining highly significant levels, might give a better repre-

resentation of the humidity profile where its fluctuations are most important. With this in mind all previous runs were recalculated using the same initial conditions and cloud base height, but changing the input levels of the sounding. The results were that in all cases tested cloud growth from a sounding with a more even distribution of input levels with height was greater than from a sounding containing more lower input levels. Figures 12 through 17 illustrate some of the calculated differences. Table 2 gives a complete list of the differences for the cases tested.

To explain this the soundings, as the computer interpreted them, were plotted on pseudo-adiabatic diagrams and compared. The morning sounding on 15 July 69 is shown in Figure 18. The solid lines are temperatures and dewpoints as the computer interprets them given an approximately even distribution of levels with height; the dotted lines are temperatures and dewpoints interpreted from a sounding with more lower levels. Examination of Figure 18 shows that the addition of more lower levels in the sounding reduces the error from interpolation in the important low layers. The sounding is much dryer than that found from an even distribution with height and also contains a more stable layer at upper levels. The combination of these features in this sounding would tend to cause the model to suppress cloud growth more than in the case where the model is using a sounding with an even distribution.

Again, with the afternoon sounding on 15 July 69, the interpolation of the sounding with levels more evenly distributed with height gives a much more moist sounding than is found when more lower levels are used. See Figure 19. The temperature profiles are much the same except for a shallow stable layer near 460 mb for the sounding containing more lower levels. Nevertheless, the moisture difference between the two interpretations of the same sounding is significant enough to cause cloud top differences.

The two interpretations of the 0700 MST radiosonde on 22 July 69 are quite different, as seen in Figure 20. Again, more moisture is introduced by the interpolation procedure for the even distribution of levels with height interpretation, but also the temperature profile is less stable for this case. The introduction of more lower levels to be input allowed a shallow stable layer near 560 mb to be detected along with greater stability at upper levels. So once again it is reasonable for greater growth to occur in the case of more available moisture and a less stable temperature profile.

The actual differences in cloud tops from the two sounding interpretations, for various initial conditions, are illustrated in Table 2. Cloud top differences were greatest when the base was low, as the LCLs for the morning soundings were; lesser differences were exhibited when cloud bases were high.

The region most sensitive to small changes in envi-

ronmental conditions seemed to be from cloud base to approximately 500 mb. If sounding interpretations differed in low levels and very high levels and cloud base was chosen above the low level differences, little variation in predicted cloud size occurred. The morning sounding on 15 July 69 with the CCL as cloud base level is a case in point.

For 1300 MST on 15 July 69 using the LCL of 666 mb as cloud base the range in cloud top differences was zero to 4800 feet. But the use of the CCL of 656 mb, only 10 mb higher, as cloud base for the same sounding interpretation gives a range of 700 feet to 1400 feet, considerably less. This is explained by noticing on Figure 19 that the choice of a base at 656 mb reduces the excess moisture produced by the interpolation procedure for the even distribution with height sounding interpretation to one-third to one-half of the amount present with base at the LCL.

The cloud top differences for the 0700 MST radiosonde on 22 July 69 were 1500 feet to 5400 feet with the base at the 850 mb LCL and 400 feet to 3600 feet with the base at the 760 mb CCL. These values exhibit a less marked difference between the case with the LCL as cloud base and the case with the CCL as cloud base; this is due to more stability and less moisture distributed throughout the sounding with more lower input levels than for the same sounding with a more even distribution of input levels. Thus the choice of a higher cloud base level does not avoid most of the dissimilarities of the two interpretations of the

soundings, as was true in the two previous cases.

For the three soundings used in this section, the choice of more lower input levels caused cloud top heights to be consistently lower than did the choice of levels more evenly distributed with height. The explanation for this was nearly the same in all cases: more moisture than was actually present was introduced by the interpolation procedure when low sounding levels were farther apart. Conceivably, the reverse could be true, presumably with the opposite result. In any case, it is evident that for very small changes in atmospheric conditions in a vertical column the model can produce quite different clouds. However, this may be a property of the real atmosphere as well.

Sensitivity to choice of initial radius and vertical velocity

Along with other initial specifications, the plume model requires an initial radius and vertical velocity at cloud base to be input. In addition to the aforementioned sensitivities, the model was found to be quite sensitive to these initial conditions.

It was decided that a very wide range of combinations of initial radii and vertical velocities would be input to test the model's capabilities and to determine the proper range on the variables to be used when computing clouds to be compared with measured clouds. The radii used were 100, 500, 1000, 2000, 10,000, and 1,000,000 meters. Vertical

velocities were 0.5, 1, 2, 5, and 10 meters per second. All thirty combinations of these variables were computed for the morning sounding of 15 July 69 with both the LCL and the CCL as cloud base and for the afternoon sounding of the same day with the LCL as cloud base. Figures 21 through 29 are examples of the vertical profiles which result.

In all cases tested the most realistic profiles were obtained with the initial conditions of 500,2; 1000,1; 1000,2; 2000,1 and 2000,2. For certain soundings and bases other combinations gave reasonable profiles, but the above five were consistently acceptable. After an examination of the clouds in the photographs it was decided that the four combinations 1000,1; 1000,2; 2000,1 and 2000,2 would be used. Of course, there was a wide range in predicted cloud top heights with all combinations, including the above four.

Very small initial radii and vertical velocities often exhibited vertical profiles with a sharp decrease and then increase of radius with height. The vertical velocity then reached unrealistically high values in low levels, corresponding to the point at which the radius became so small. It is unclear exactly what feature of the model produces this, but it is thought that possibly the treatment of entrainment causes such behavior, since a very large proportion of such a small cloud would be entraining.

In cases where a large initial vertical velocity was

coupled with a relatively small initial radius, the computed plume radius increased slightly, decreased and then increased again. Some simple calculations made with a similar but dry model suggest this is natural behavior for the plume, given an unstable sounding. In fact, dry calculations suggested this may be natural behavior in all cases, though it does not seem to be the result in most of the other cases tested. It was thought that perhaps the radius did increase initially, however slightly, in all cases but that it decreased again quite rapidly, before the first level of print-out was reached. To check this, runs were made with the number of interpolation points between sounding input levels increased, with the values of variables printed out for each interpolation point. There was no evidence, however, that the radius initially does increase with the wet model, as was suggested by hand calculations with the dry model.

In a few cases, the plume radius at the end of upward motion increased to extremely large values. The vertical velocity was very small in these cases. The large radii would be produced by the requirement that the mass flux be finite. As the vertical velocity approaches zero, the radius must approach infinity due to the mass flux constraint.

A basic assumption made in formulating the plume model is that the plume is tall and narrow. Scaling assumptions are made accordingly, so the use of a very large radius is inappropriate. Nevertheless, out of curiosity

a synoptic scale radius, one million meters, was input. Surprisingly, realistic vertical profiles resulted with most initial vertical velocities. Regardless of the initial vertical velocity, the clouds with the large initial radius all grew to the same height. Figures 30, 31 and 32 illustrate the three test cases. A possible explanation of this is as follows. A cloud with a large radius is affected very little by entrainment. A great deal of energy is contained in such a cloud, derived predominantly from the latent heats of condensation and freezing. The initial impulse created by a specified vertical velocity at cloud base is a very small proportion of the total energy of the cloud, and cloud growth would therefore be governed by latent heat release, which is the same for a given sounding and cloud base height. Thus, all clouds with the large initial radius would reach the same height.

Ten thousand meters was also input as an initial radius. Figure 33 is an example of the computed profiles. Cloud growth was similar to that for one million meters, but with a slight variation in cloud tops with input vertical velocity. A similar explanation would apply to this case.

Sensitivity to humidity profile

It is well known that the dewpoint sensor in radiosonde equipment ceases to give representative values at high levels. Since some of the sounding input levels

were always above the level at which dewpoints no longer were available, the question arose of what value to input in lieu of a reading. The plume model is programmed to receive temperature and dewpoint data in the same coded form as it is relayed on National Weather Service teletype circuits, that is, a coded five digit group with temperature and dewpoint depression. It was thought that the layers for which dewpoint measurements were not available contained only a small percentage of the total moisture in the plume, so the sounding was dried out in these layers by inserting a 99 for dewpoint depression in the code group. However, to be certain the effect of the moisture in these upper layers was minimal a check seemed advisable. Runs were made for comparison that were identical to the dried out runs except that a constant relative humidity, equal to that at the last known level, was maintained for the remainder of the sounding.

The results showed no change in any variable throughout the vertical extent of the plume except for the radius at the end of upward motion, in a few cases. The vapor, liquid and solid water contents were the same whether the humidity was constant or the sounding was dried out above the last known dewpoint data point. The differences in radii were negligible, ranging from zero to only $7\frac{1}{2}$ meters. Possibly this was a result of the integration technique. In any case, the plume does not seem at all sensitive to humidity variations in the upper levels.

6. Model predictions compared with observed growth

Having investigated the limitations of the plume model, it remains to predict cloud development with it and compare the results to what actually formed in the atmosphere. Photogrammetric techniques were employed to obtain measurements of real clouds, but some problems were encountered in implementing the techniques. Variability was encountered in many aspects of this study, e.g., in the plume model calculations, in photogrammetric measurements, in the real atmosphere. The question is whether the amount of variability displayed is physically realistic and comparable to that of the real atmosphere.

Description of photogrammetric techniques

The heights of cloud bases and tops were desired for the three test days; they were obtained from simultaneous stereo photographs taken every few minutes. The cameras were located at the ends of a baseline oriented perpendicular to the azimuth 151.28° from true north. The distance between cameras was 7894 feet, and the cameras were mounted so that the focal plane was perpendicular to the horizontal.

The photogrammetric procedure is based on the principle of parallax measurement. The range Y of a point in space is determined from the following equations for the normal case of photogrammetry. These equations assume the cameras' optical axes were approximately parallel and

oriented horizontally.

$$Y = \frac{B_x}{f} f$$

$$X = \frac{B_x}{f} x'$$

$$Z = \frac{B_x}{f} z'$$

where B_x is the baseline distance perpendicular to the camera axis, f is the focal length (assumed the same for both cameras) and p is the parallax. Figure 34 illustrates the geometry for parallax in the normal case.

$$p = x' - x''$$

where x' and x'' are shown in Figure 34. z' is obtained in a similar manner. The values x' and z' are found with respect to fiducial lines on the reference photograph, which in the case illustrated is that photograph taken with the north camera. The coordinates X and Z are positive eastward and upward, respectively.

The above equations were used for measurements on 22 July 69 and 25 July 69. Calculations made of distances and heights of peaks with known values and known azimuths showed the optical axes of the cameras to be very nearly parallel on these days.

Triangulations done from the 15 July 69 photographs revealed the optical axis of the north camera to be oriented 1.2° to the right of the perpendicular to the baseline.

Figure 35 illustrates the parallax geometry involved. The following equations include a correction for this source of error.

$$\tan \beta = \frac{X_{N1}}{f}$$

$$\tan (\beta + \omega) = \frac{X_{N0}}{f}$$

$$p = X_{N0} - X_{S0} = f \tan (\beta + \omega) - X_{S0} = f \left[\frac{\tan \beta + \tan \omega}{1 - \tan \beta \tan \omega} \right] - X_{S0}$$

where β , X_{N0} , X_{S0} and X_{N1} are shown in Figure 35 and $\omega = 1.2^\circ$. In this case the reference photograph is from the south camera.

$$Y_s = \frac{f B_x}{f}$$

$$Z_s = \frac{Y_0}{f} Z_{S0}$$

There are several sources of error in these measurements. The camera orientation can possess tip, tilt and swing, some of which are quite difficult to detect. The focal lengths of the cameras were well matched, and the increase of precision obtainable by correction for the differences was not deemed significant. Error in the measurements presented in this thesis was estimated to be of the order of a few percent. To minimize this an average of cloud base heights was used in the final calculations with the plume model. Numerical calculations were carried out with as many significant digits as

measurements allowed.

Comparison of predicted and measured cloud base heights

Using photogrammetric techniques the heights of cloud bases and tops were measured from photographs taken on the three test days. Table 3 lists the results of these measurements.

The measured base heights increased slightly with time on each day. Figure 36 is a plot of cloud base height with time. Considerable scatter exists, but what curve fitting was possible seemed to indicate an increase in cloud base height with time on all three days. This was probably a result of heating over the mountains which would slightly modify atmospheric conditions in the vicinity of the cloud. Clouds that formed previously in a particular area would also contribute to a redistribution of heat and moisture and an alteration in the level at which the formation of new clouds would occur.

The heights of cloud bases on a particular day were found to vary by as much as 2000 feet, but generally varied by approximately 1000 feet. At any given time the variation was one thousand feet or less. Over the plains it has been noted that cloud bases generally form at nearly the same level. Although the measurements in this investigation suggest that this is not true over the mountains, the variation could easily be attributed to error incurred by the crudity of the photogrammetric techniques employed here. However, it seems entirely possible and even probable that

there would indeed be variation in cloud base heights over mountains. The forced mechanical lifting of the terrain and particularly an elevated heat source with substantial horizontal variation would undoubtedly produce horizontal variation in atmospheric conditions sufficient to cause cloud formation at different heights. Nevertheless, since it is not known whether the discrepancies encountered were real or a result of error in measurements, an average of measured cloud bases was taken and is listed in Table 3.

It is seen that the average base for 15 July 69 was 705 mb. However, one of the cloud base measurements for that day was considerably lower than all other measured bases, as the cloud considered was over the plains west of the mountains. It was decided that this measurement was not representative of bases over mountains, and it was not included in a new base average calculation. The average base for this date was recalculated to be 679 mb, which is slightly below the morning CCL of 664 mb, but well above the LCL of 825 mb. The average base was below both the 666 mb LCL and the 656 mb CCL of the afternoon sounding.

On 22 July 69 the average measured base was 733 mb, which was above the 850 mb LCL and the 760 mb CCL of the morning sounding. The average base was below both the LCL of 680 mb and the CCL of 654 mb of the afternoon sounding.

For 25 July 69 the average base was only 1 mb higher than the morning CCL of 688 mb. It was higher than the

morning LCL of 783 mb and lower than the afternoon LCL/CCL of 653 mb.

It is seen that in all cases the average measured bases were quite near the CCL of the morning sounding and lower than the LCL or CCL of the afternoon sounding. This suggests that the primary factor contributing to the convection being studied is surface heating, although the simple process by which the CCL is obtained may not be entirely appropriate over mountainous terrain. Nevertheless, previous studies over similar isolated peaks have suggested that heating is the primary process contributing to convective development and that lifting is minimal due to air flow around rather than over the peaks.

Comparison of predicted and measured cloud top heights

The heights of the measured cloud tops varied substantially for each day. For comparison clouds were computed for each day from the morning and afternoon soundings, using the average measured cloud bases and four sets of initial conditions. The vertical profiles for each case are shown in Figures 37 through 42. The results appear in Table 4. An examination of this table reveals that initial radius 2000 m and vertical velocity 2 mps consistently over-predicted cloud top heights. Therefore, consideration was made of the remaining predictions, excluding those made with 2000 m and 2 mps. The justification for this is that the choice of initial conditions is somewhat arbitrary

anyway, and the values of 2000 m and 2 mps may be too large.

Looking only at clouds that formed over the mountains, measured tops ranged from 14,100 feet to 23,700 feet on 15 July 69. From the morning sounding computed cloud tops ranged from 21,800 feet to 30,000 feet; the afternoon sounding gave a range from 19,400 feet to 25,300 feet.

For 22 July 69 measured tops were 11,900 feet to 34,100 feet. Computed tops were 24,400 feet to 36,200 feet from the morning radiosonde and 22,200 feet to 35,600 feet from the afternoon sounding.

From the 25 July 69 photographs, cloud tops were found to vary from 13,500 feet to 22,400 feet. Computed tops from the morning sounding were 19,700 feet to 21,000 feet and 19,300 feet to 22,300 feet with the afternoon sounding.

Some of the small clouds measured are not duplicated by computation. It is known and has been previously discussed that unrealistic profiles are obtained with small initial conditions. However, the measured small clouds were obviously in the initial stage of development, while the plume model assumes the cloud is steady-state and in the mature stage of development. Therefore, this model could not be expected to predict the heights of such infant clouds.

In the range of medium and large clouds relative to a particular day, the model predicts quite well with both the morning and afternoon soundings. In general,

cloud tops produced by the real atmosphere correspond closely to those produced by the plume model. For example, on 22 July 69 the larger clouds' tops were predominantly in the 25,000 to 35,000 foot range. The model produced cloud tops in this range quite faithfully. An even more striking example is the case of 25 July 69. The larger clouds ranged from 17,000 feet to 22,000 feet. Predicted clouds ranged from 19,000 feet to 22,000 feet.

Conclusions and Recommendations

It has been shown that the entraining convective plume model used in this research is quite sensitive to a variety of factors, and that the choice of these factors has a direct effect on the outcome of a comparison of model clouds with observed clouds.

Using an identical sounding and initial radius and vertical velocity the plume model produces cloud tops that differ by thousands of feet when different cloud base levels are chosen. A difference of only 10 mb in cloud base can result in largely different cloud tops.

Cloud growth is also highly dependent on the choice of sounding levels to be input. In the cases tested the use of more lower levels, to gain a better representation of the low level humidity profile, produced consistently smaller clouds than did a sounding with a more even distribution of levels with height, all other input parameters being equal. An examination of the two computer

interpretations of the sounding revealed that the interpolation procedure caused more moisture to be present in low levels when an even distribution was input. Although this particular result was found in all cases tested, the opposite could easily occur.

The plume model was tested with a wide range of initial radii and vertical velocities at cloud base. For very small initial conditions unrealistic vertical profiles and vertical velocities were produced. Very large initial radii, although violating the scaling assumptions made in formulating the plume equations, nevertheless gave somewhat realistic profiles. However, the initial radii and velocities of 1000,1; 2000,1; 1000,2 and 2000,2 were judged most applicable to the convection being studied.

A test of the model's sensitivity to the humidity input above the level where dewpoint information was no longer available showed virtually no change in the output, whether the sounding was dried out or maintained at a constant relative humidity. Evidently the amount of moisture above that level is so small a percentage of the total moisture that cloud development is independent of it.

Measured cloud bases were found to increase with time on all three days, probably a result of surface heating. The variability of cloud base heights at any given time on a particular day was one thousand feet or less. Error in photogrammetric measurements was sufficient to account for this, but it is also reasonable to assume that

variation in cloud base height does exist over mountainous terrain, as horizontal variation in surface heating is present. Actual cloud bases were found to be quite near the convective condensation level of the morning sounding. Bases in all cases were below both the LCL and the CCL of the afternoon soundings. These findings suggest that an elevated heat source is dominant in determining cloud base height and the effect of lifting is minimal. Other studies over isolated peaks have obtained similar results.

Cloud top heights were predicted using the four sets of initial conditions previously mentioned and the average measured cloud base heights. Initial radius 2000 m and vertical velocity 2 mps were found to over-predict. The remaining predictions corresponded closely with measured heights for the medium and large clouds observed on each day. The model did not predict cloud top heights for smaller clouds, as they were not observed to be in a mature stage of development.

For more conclusive results it is recommended that more than one type of convection model be used for purposes of prediction. Perhaps a "field of motion" model and an "entity" model should both be used and their results compared as well as a comparison with observed clouds. Of course the sensitivities of any model used for such purposes must be thoroughly explored.

The photogrammetric techniques are subject to considerable error and many measurements should be made to

obtain a large sample. More sophisticated techniques should be employed than were possible for this thesis, such as a computer program that corrects for camera tip, tilt and swing, as discussed by Glass and Carlson (1963).

The use of the above models and techniques could presumably serve to further clarify the nature of convection.

List of Tables and Figures

Table

1. Cloud top differences between LCL cloud base and CCL cloud base
2. Cloud top differences between sounding with even distribution with height and one with more lower levels
3. Photogrammetrically measured cloud bases and tops
4. Comparison of measured cloud tops and computed cloud tops

Figure

1. Map of Organ Mountains and vicinity
2. Radiosonde soundings, 15 July 69, 0500 MST and 1300 MST
3. Radiosonde soundings, 22 July 69, 0700 MST and 1300 MST
4. Radiosonde soundings, 25 July 69, 0500 MST and 1300 MST
5. Plume profiles with bases at LCL and CCL for 15 July 69 0500 MST, initial conditions 1000,1 and 2000,1
6. Plume profiles with bases at LCL and CCL for 15 July 69 0500 MST, initial conditions 1000,2 and 2000,2
7. Plume profiles with bases at LCL and CCL for 15 July 69 1300 MST, initial conditions 1000,1 and 2000,1
8. Plume profiles with bases at LCL and CCL for 15 July 69 1300 MST, initial conditions 1000,2 and 2000,2
9. Plume profiles with bases at LCL and CCL for 22 July 69 1300 MST, initial conditions 1000,1 and 2000,1
10. Plume profiles with bases at LCL and CCL for 22 July 69 1300 MST, initial conditions 1000,2 and 2000,2
11. Computer interpretation of radiosonde sounding, 22 July 69, 1300 MST
12. Plume profiles from two computer interpretations of 15 July 69, 0500 MST sounding, base LCL, initial conditions 1000,1 and 2000,2
13. Plume profiles from two computer interpretations of 15 July 69, 0500 MST sounding, base LCL, initial condi-

- tions 2000,1 and 1000,2
14. Plume profiles from two computer interpretations of 15 July 69, 1300 MST sounding, base CCL, initial conditions 1000,1 and 2000,2
 15. Plume profiles from two computer interpretations of 15 July 69, 1300 MST sounding, base CCL, initial conditions 2000,1 and 1000,2
 16. Plume profiles from two computer interpretations of 22 July 69, 0700 MST sounding, base LCL, initial conditions 1000,1 and 2000,2
 17. Plume profiles from two computer interpretations of 22 July 69, 0700 MST sounding, base LCL, initial conditions 2000,1 and 1000,2
 18. Two computer interpretations of 15 July 69, 0500 MST radiosonde sounding
 19. Two computer interpretations of 15 July 69, 1300 MST radiosonde sounding
 20. Two computer interpretations of 22 July 69, 0700 MST radiosonde sounding
 21. Plume profiles, 15 July 69, 0500 MST, base LCL, initial conditions 100,0.5; 500,0.5; 1000,0.5; 2000,0.5
 22. Plume profiles, 15 July 69, 0500 MST, base LCL, initial conditions 100,5; 500,5 and 1000,5
 23. Plume profiles, 15 July 69, 0500 MST, base LCL, initial conditions 100,10; 500,10 and 1000,10
 24. Plume profiles, 15 July 69, 0500 MST, base CCL, initial conditions 100,10; 500,10; 1000,10 and 2000,5
 25. Plume profiles, 15 July 69, 1300 MST, base LCL, initial conditions 100,0.5; 500,0.5; 1000,0.5; 2000,0.5
 26. Plume profiles, 15 July 69, 1300 MST, base LCL, initial conditions 100,1; 500,1; 1000,1 and 2000,1
 27. Plume profiles, 15 July 69, 1300 MST, base LCL, initial conditions 100,2; 500,2; 1000,2 and 100,5
 28. Plume profiles, 15 July 69, 1300 MST, base LCL, initial conditions 500,5; 100,10 and 500,10
 29. Plume profiles, 15 July 69, 1300 MST, base LCL, initial conditions 2000,2; 1000,5; 2000,5 and 1000,10

30. Plume profiles, 15 July 69, 0500 MST, base LCL, initial conditions 1,000,000 radius and 0.5, 1, 2, 5, 10 vertical velocity
31. Plume profiles, 15 July 69, 0500 MST, base CCL, initial conditions 1,000,000 radius and 0.5, 1, 2, 5, 10 vertical velocity
32. Plume profiles, 15 July 69, 1300 MST, base LCL, initial conditions 1,000,000 radius and 0.5, 1, 2, 5, 10 vertical velocity
33. Plume profiles, 15 July 69, 1300 MST, base LCL, initial conditions 10,000 radius and 0.5, 1, 2, 5, 10 vertical velocity
34. Parallax geometry for normal case
35. Parallax geometry, north camera 1.2° to right of perpendicular to baseline
36. Cloud base height versus time from photogrammetry
37. Plume profiles, 15 July 69, 0500 MST, base 679 mb, initial conditions 1000,1; 2000,1; 1000,2 and 2000,2
38. Plume profiles, 15 July 69, 1300 MST, base 679 mb, initial conditions 1000,1; 2000,1; 1000,2 and 2000,2
39. Plume profiles, 22 July 69, 0700 MST, base 733 mb, initial conditions 1000,1; 2000,1; 1000,2 and 2000,2
40. Plume profiles, 22 July 69, 1300 MST, base 733 mb, initial conditions 1000,1; 2000,1; 1000,2 and 2000,2
41. Plume profiles, 25 July 69, 0500 MST, base 687 mb, initial conditions 1000,1; 2000,1; 1000,2 and 2000,2
42. Plume profiles, 25 July 69, 1300 MST, base 687 mb, initial conditions 1000,1; 2000,1; 1000,2 and 2000,2

Table 1

Cloud top differences between LCL cloud base and CCL cloud base

date	time	LCL and CCL	radius (m) & vert. vel. (mps)	cloud top differences (feet)
7-15-69	0500	LCL-825 CCL-664	1000,1	7500
			2000,1	9000
			1000,2	7100
			2000,2	11800
7-15-69	1300	LCL-666 CCL-656	1000,1	700
			2000,1	1900
			1000,2	700
			2000,2	2400
7-22-69	0700	LCL-850 CCL-760	1000,1	1500
			2000,1	3800
			1000,2	3500
			2000,2	5200
7-22-69	1300	LCL-680 CCL-654	1000,1	-2500
			2000,1	- 500
			1000,2	-1300
			2000,2	-3500
7-25-69	0500	LCL-783 CCL-688	1000,1	3400
			2000,1	17700
			1000,2	5900
			2000,2	19800
7-25-69	1300	LCL=CCL 653		none

Table 2

Cloud top differences between sounding with even distribution with height and one with more lower levels

date	time	base	radius (m) & vert. vel. (mps)	cloud top difference (feet)
7-15-69	0500	LCL-825	1000,1	1400
			2000,1	0
			1000,2	2200
			2000,2	3300
7-15-69	0500	CCL-664	1000,1	300
			2000,1	0
			1000,2	0
			2000,2	0
7-15-69	1300	LCL-666	1000,1	0
			2000,1	800
			1000,2	1700
			2000,2	4800
7-15-69	1300	CCL-656	1000,1	600
			2000,1	1400
			1000,2	700
			2000,2	1100
7-22-69	0700	LCL-850	1000,1	5400
			2000,1	1700
			1000,2	1500
			2000,2	3300
7-22-69	0700	CCL-760	1000,1	400
			2000,1	3600
			1000,2	2000
			2000,2	3100

Table 3

Photogrammetrically measured cloud bases and tops

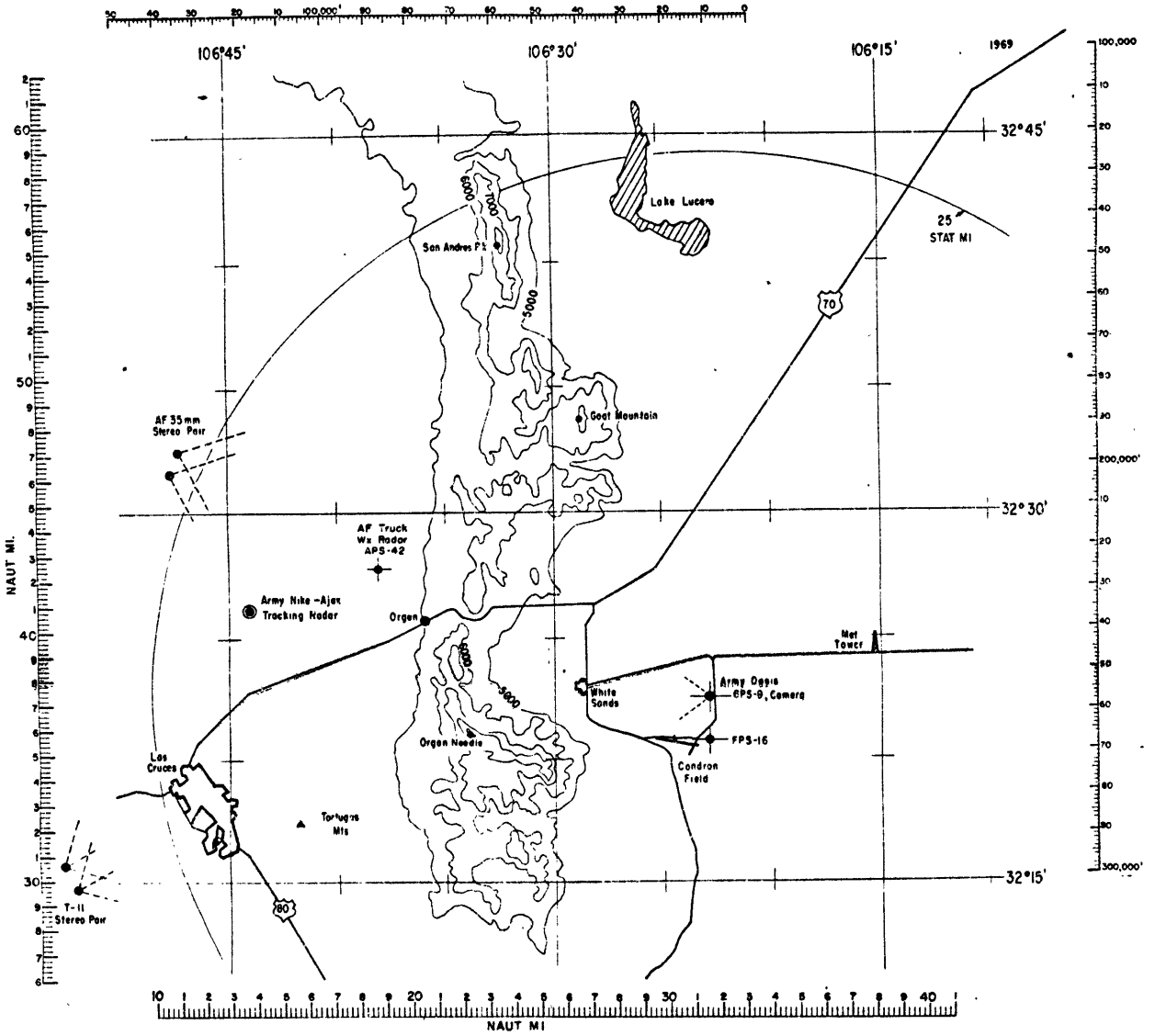
date	time	cloud base (ft)	cloud base (mb)	cloud top (ft)	range (ft)	
7-15-69	14:33	6375	810	10,661	53,000	
	16:05	11,790	666	23,691	103,000	
		11,257	681	15,461	97,000	
	16:30	9935	712	14,139	89,000	
		12,118	658	16,322	100,000	
7-22-69	16:00	8436	753	33,429	98,000	
		9108	735	32,137	130,000	
	16:15	8965	739	16,291	147,000	
		9291	730	34,064	103,000	
	16:33	9402	728	11,901	115,000	
		9028	737	26,623	90,000	
	17:20	9324	730	15,168	128,000	
		10.020	712	15,500	81,000	
	7-25-69	14:23	10,343	703	17,945	86,000
			10,782	692	20,175	110,000
14:35		11,035	685	22,435	112,000	
14:49		11,365	677	13,525	49,000	
		11,396	676	13,533	105,000	

Table 4

Comparison of measured cloud tops and computed cloud tops

date	time	measured tops (ft)	radius (m) & vert. vel. (mps)	computed tops (ft)	
				morn. sounding	aft. sounding
7-15-69	14:33	10,661	1000,1	21,800	19,400
	16:05	23,671	2000,1	30,000	25,300
		15,461	1000,2	25,100	21,300
	16:30	14,139	2000,2	33,900	33,800
16,322					
7-22-69	16:00	33,429	1000,1	24,400	22,200
		32,137	2000,1	36,200	35,600
	16:15	16,291	1000,2	29,500	26,400
		34,064	2000,2	40,100	43,100
	16:33	11,901			
		26,623			
	17:20	15,168			
15,500					
7-25-69	14:23	17,945	1000,1	19,700	19,300
		20,175	2000,1	21,000	22,300
	14:35	22,435	1000,2	20,800	21,500
	14:49	13,525	2000,2	25,000	24,200
		13,533			

Figure 1.



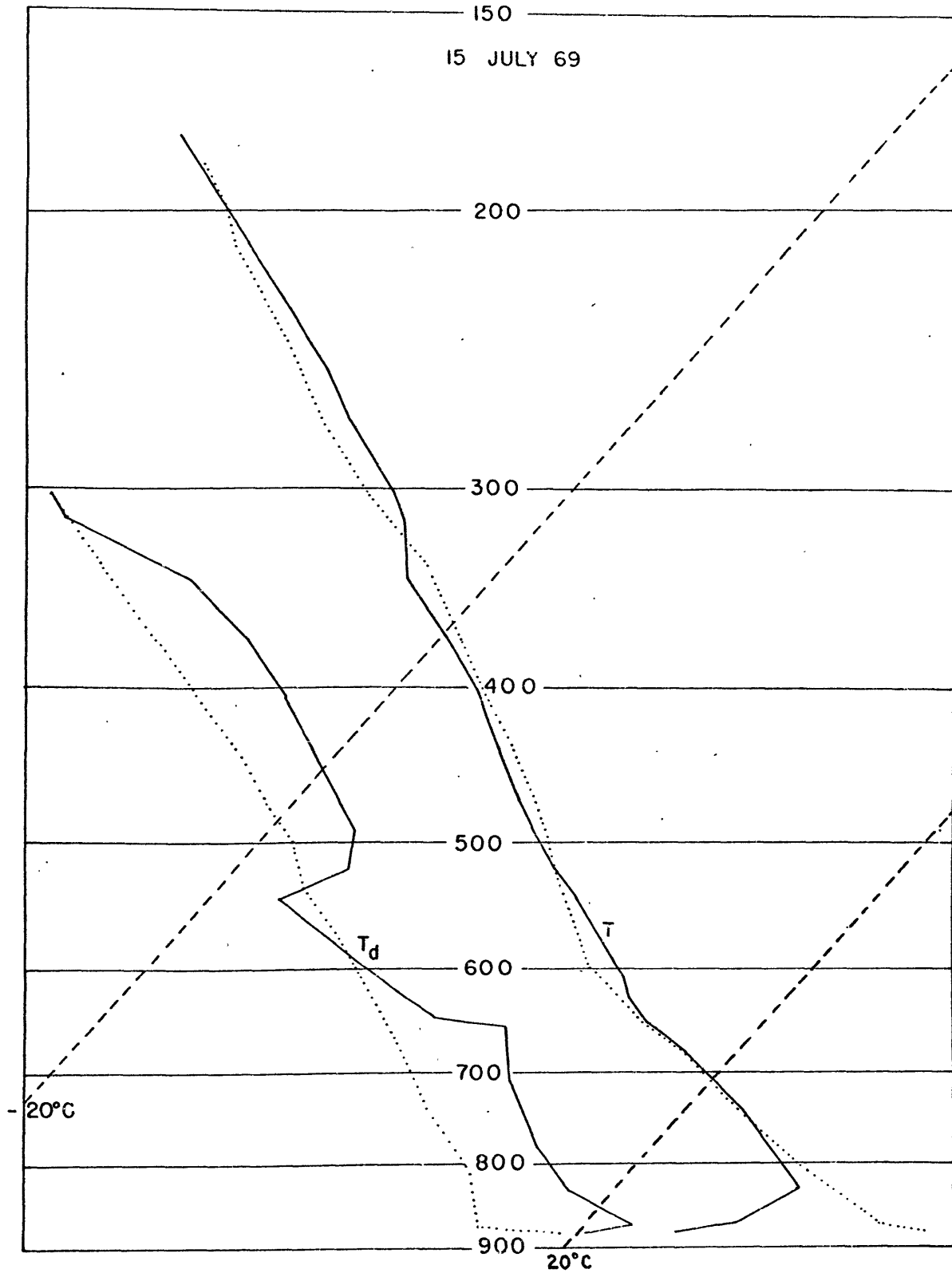


Figure 2. Radiosonde soundings, solid lines 0500 MST, dotted lines 1300 MST.

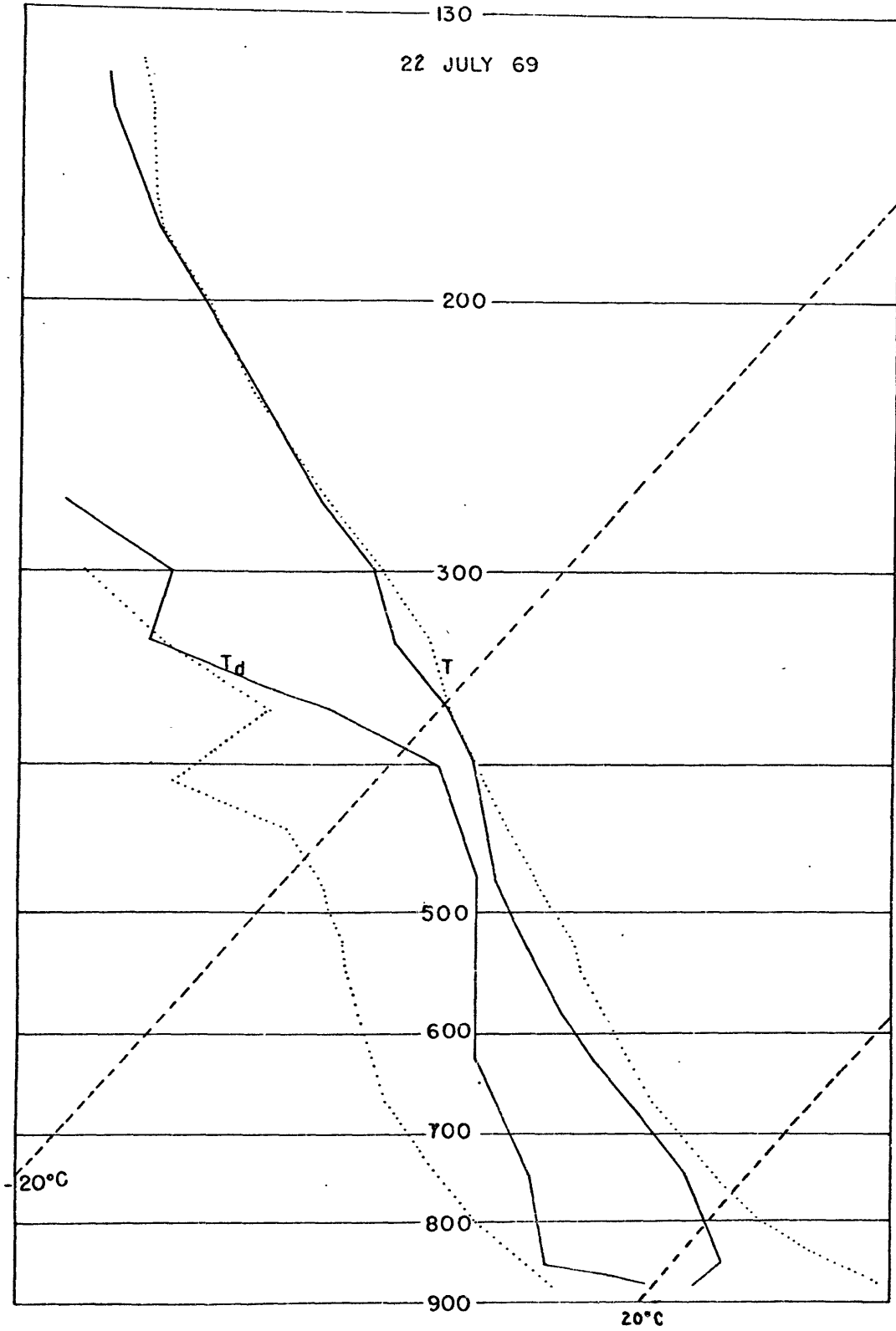


Figure 3. Radiosonde soundings, solid lines 0700 MST, dotted 1300 MST.

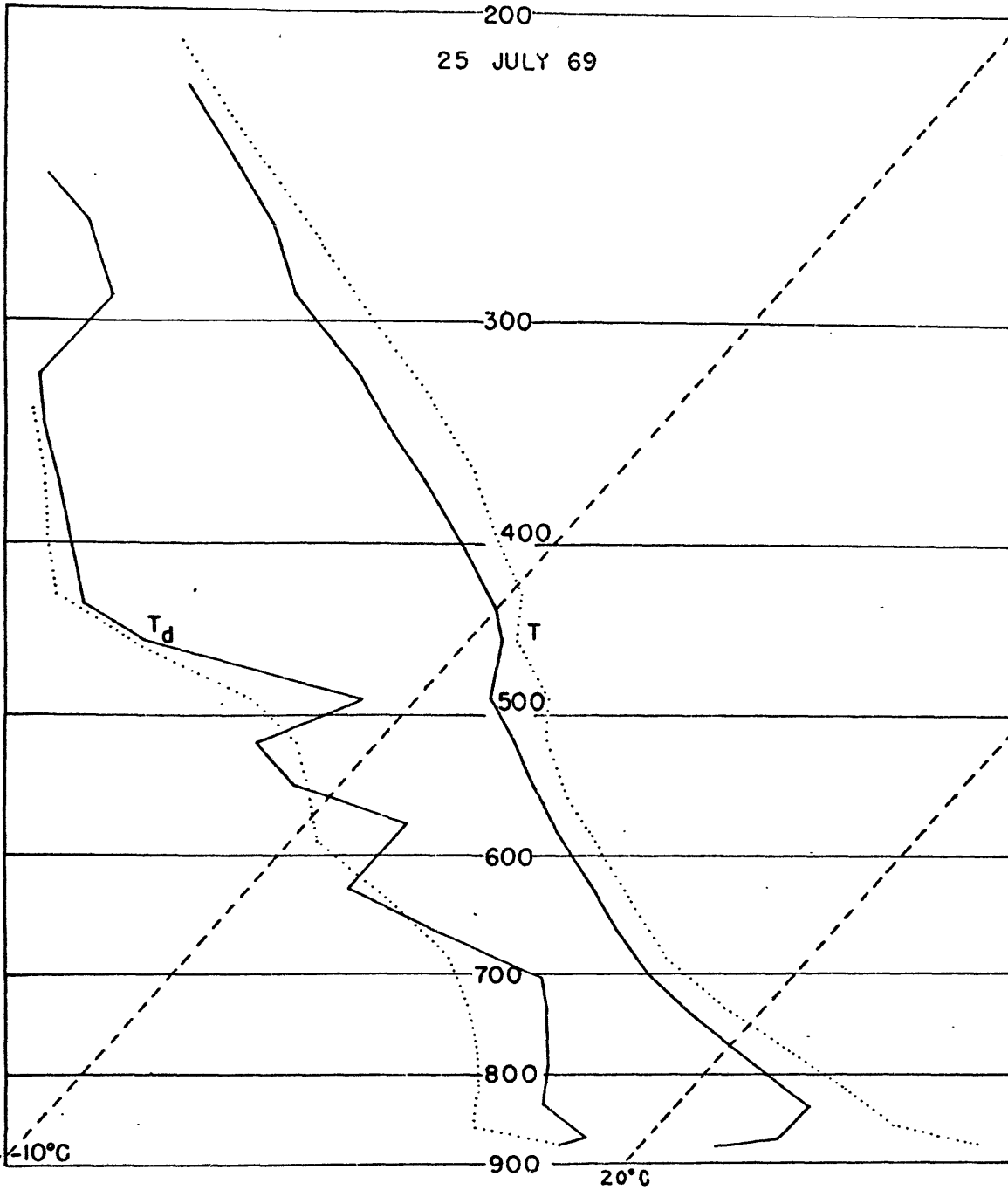


Figure 4. Radiosonde soundings, solid lines 0500 MST, dotted lines 1300 MST.

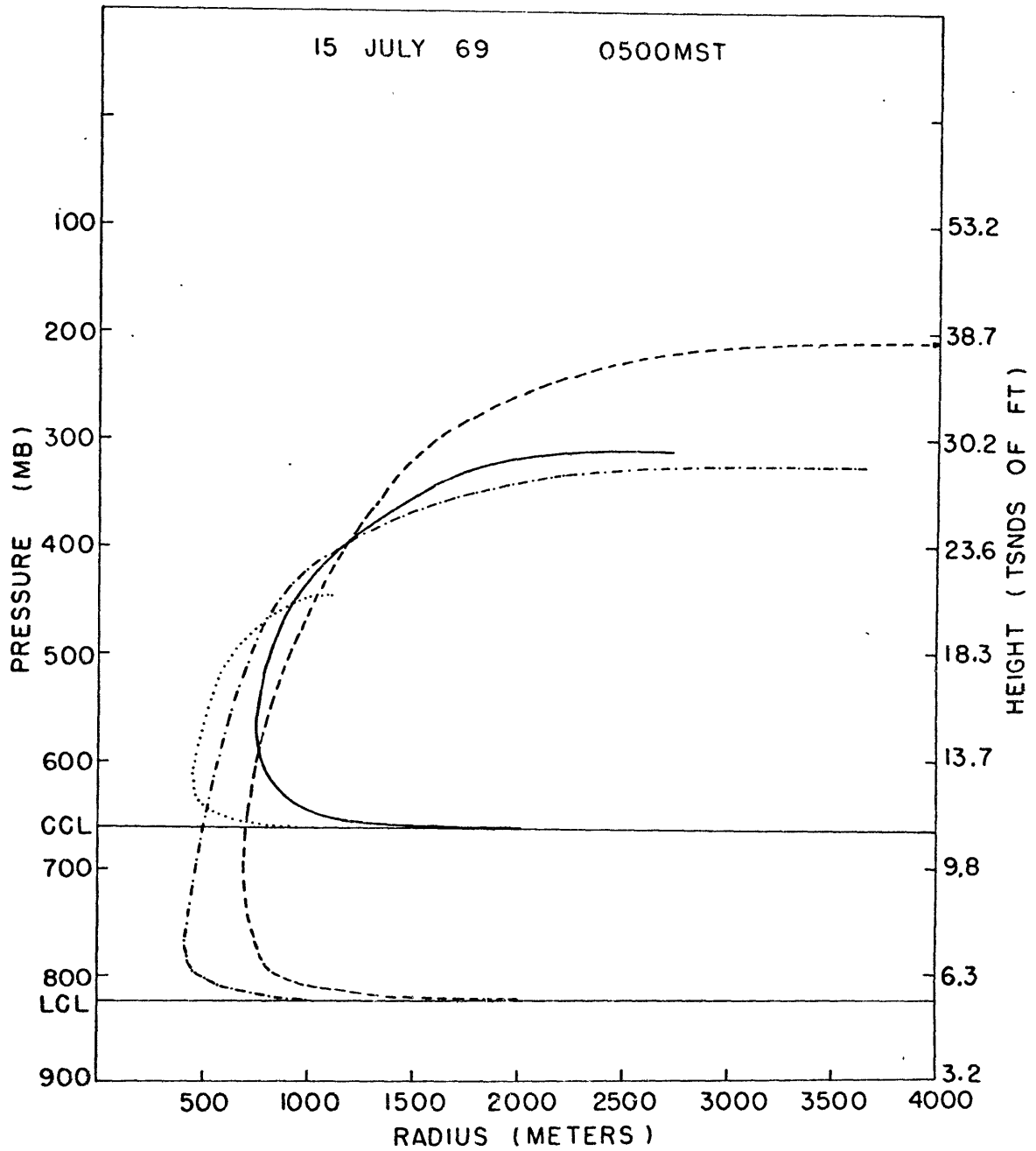


Figure 5. Plume profiles with bases at LCL and CCL, dotted line and dot-dash line initial conditions 1000,1; solid line and dashed line initial conditions 2000,1.

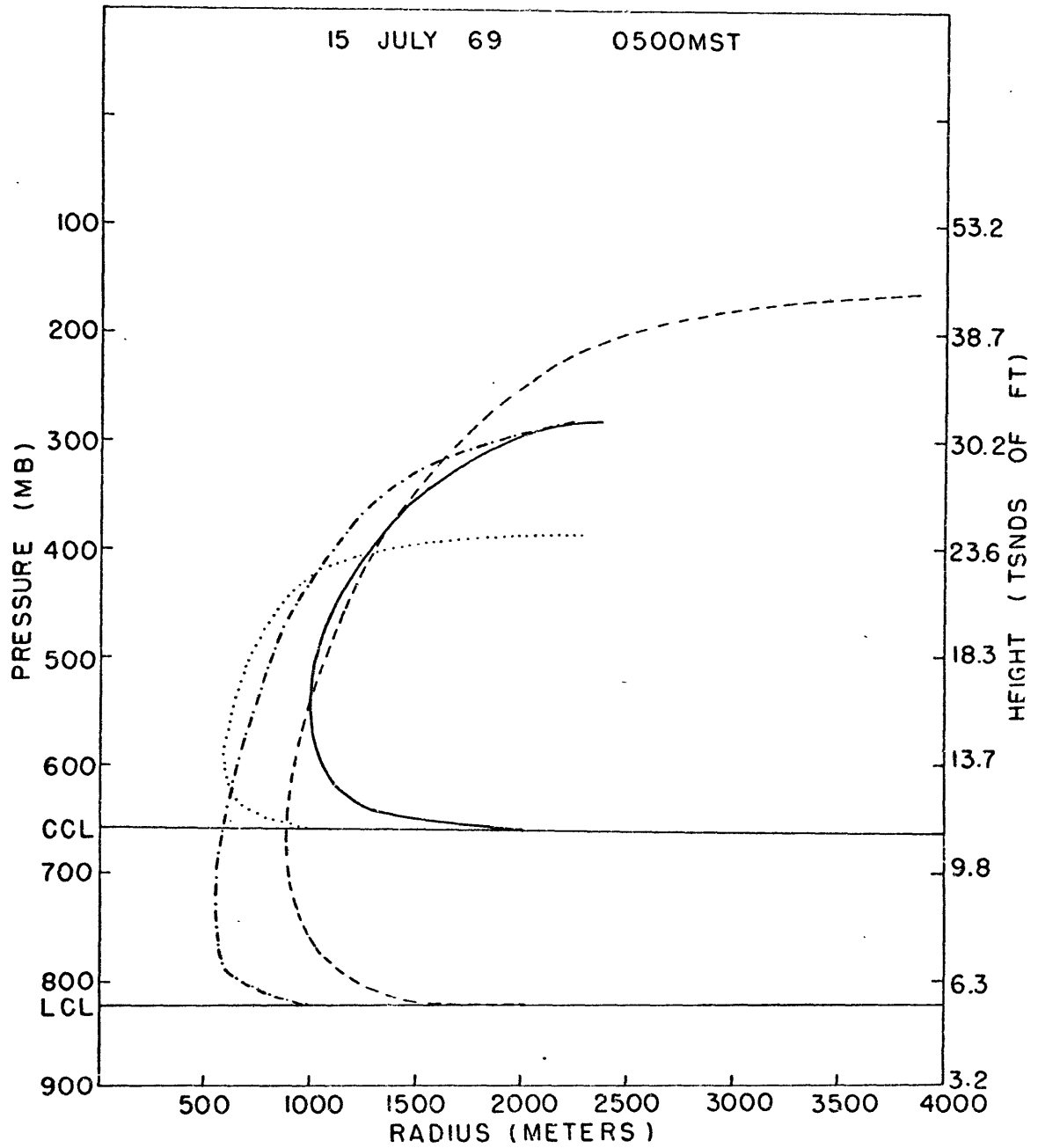


Figure 6. Plume profiles with bases at LCL and CCL, dotted line and dot-dash line initial conditions 1000,2; solid line and dashed line initial conditions 2000,2.

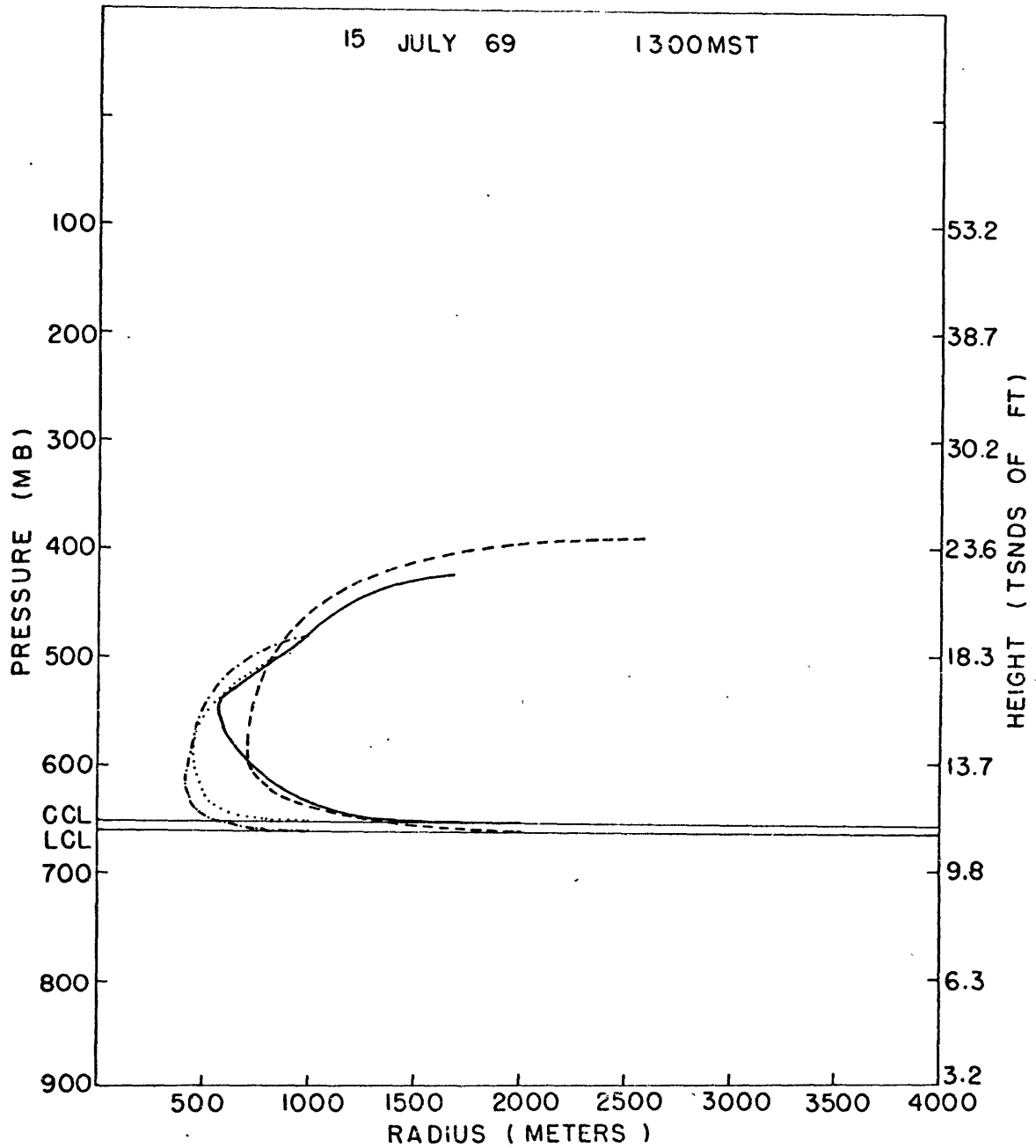


Figure 7. Plume profiles with bases at LCL and CCL, dotted line and dot-dash line initial conditions 1000,1; solid line and dashed line initial conditions 2000,1.

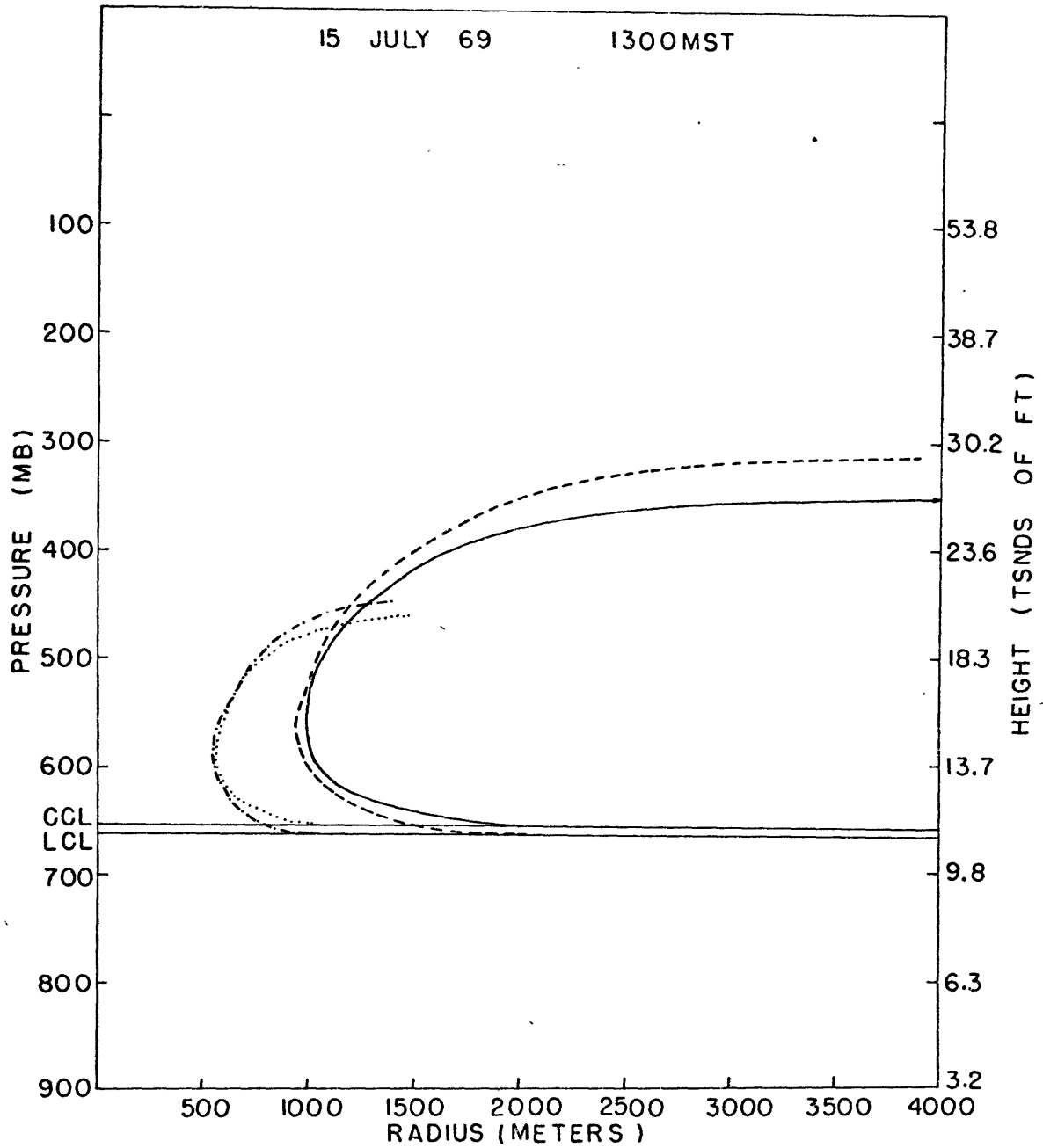


Figure 8. Plume profiles with bases at LCL and CCL, dotted line and dot-dash line initial conditions 1000,2; solid line and dashed line initial conditions 2000,2.

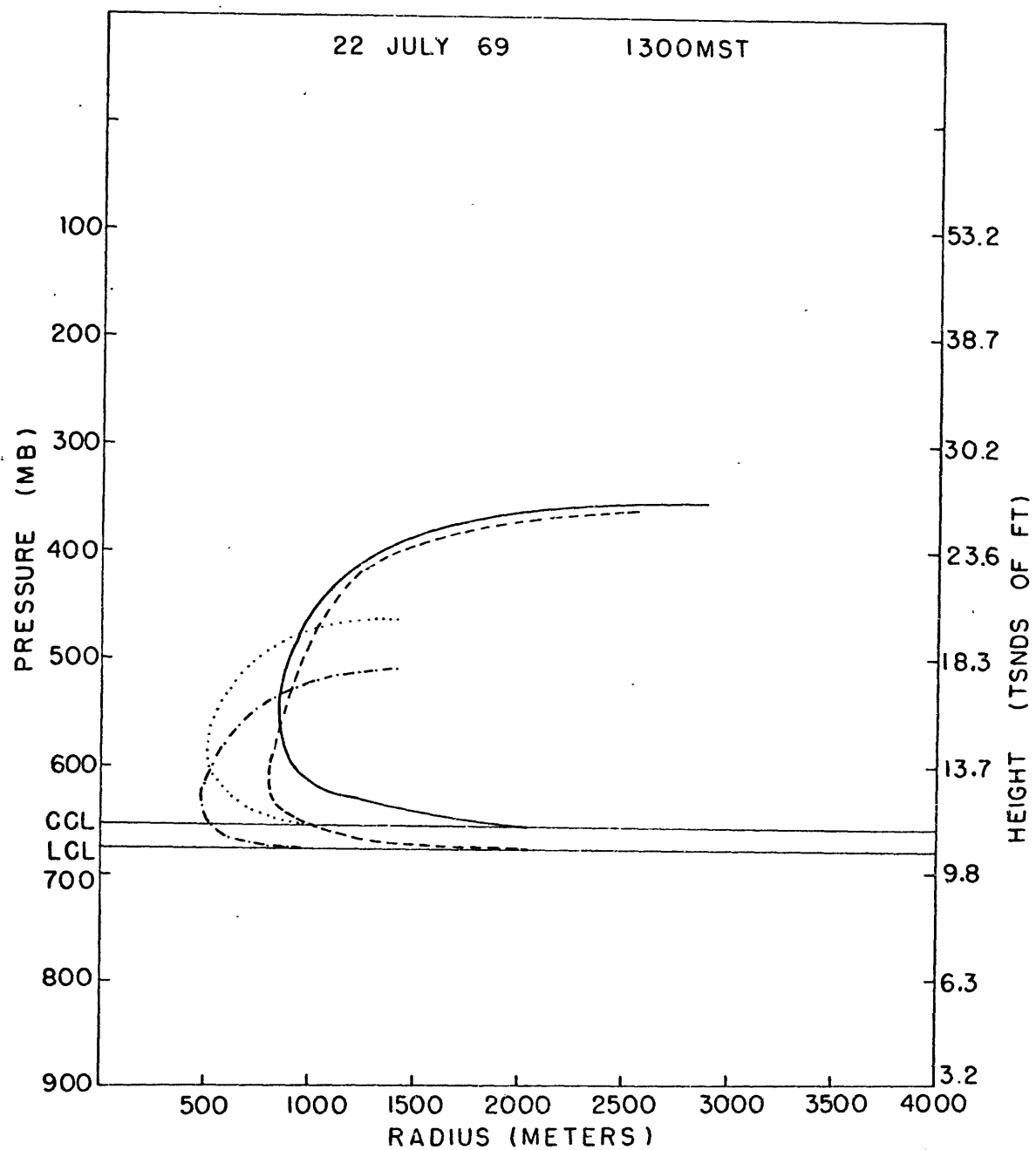


Figure 9. Plume profiles with bases at LCL and CCL, dotted line and dot-dash line initial conditions 1000,1; solid line and dashed line initial conditions 2000,1.

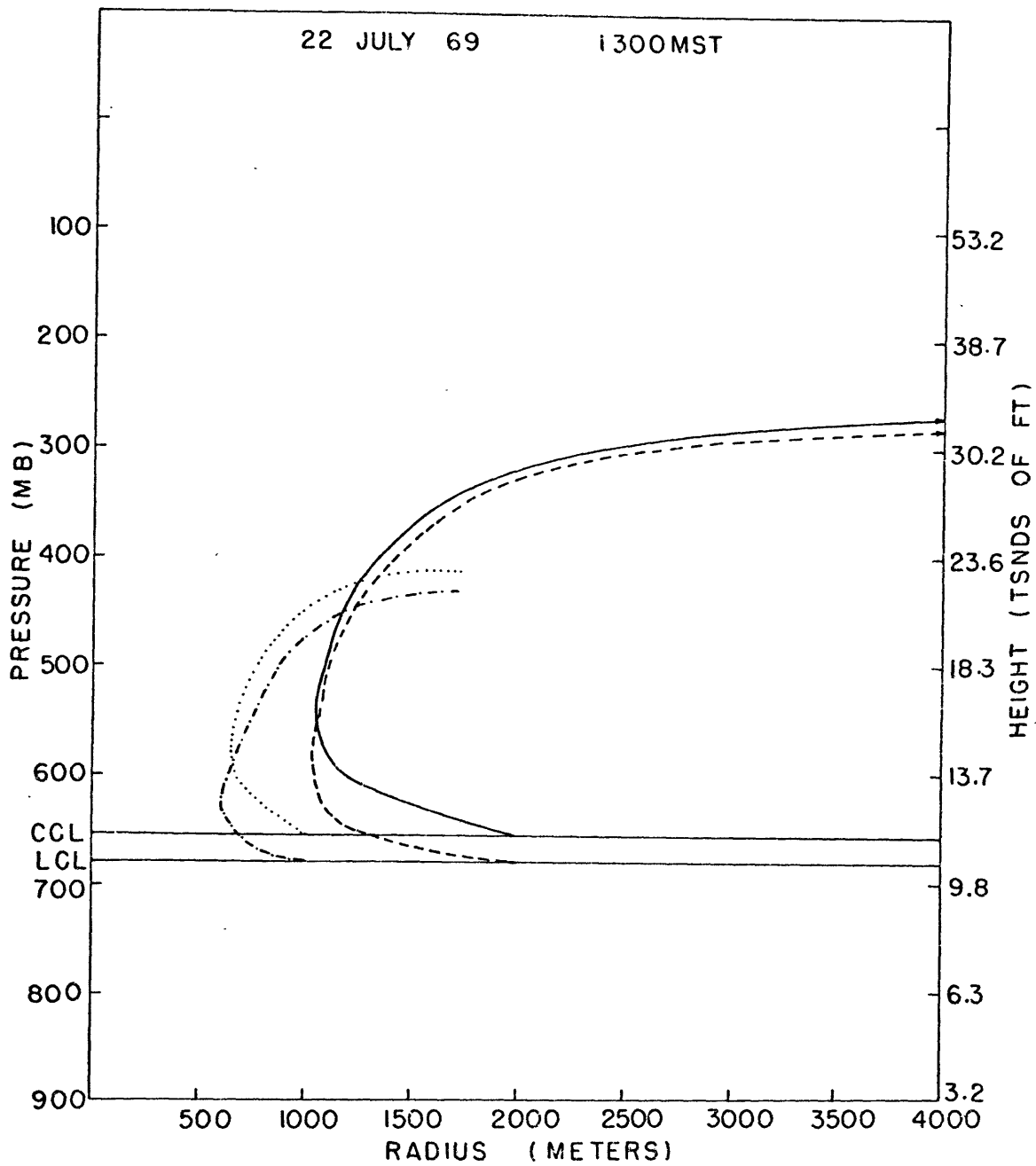


Figure 10. Plume profiles with bases at LCL and CCL, dotted line and dot-dash line initial conditions 1000,2; solid line and dashed line initial conditions 2000,2.

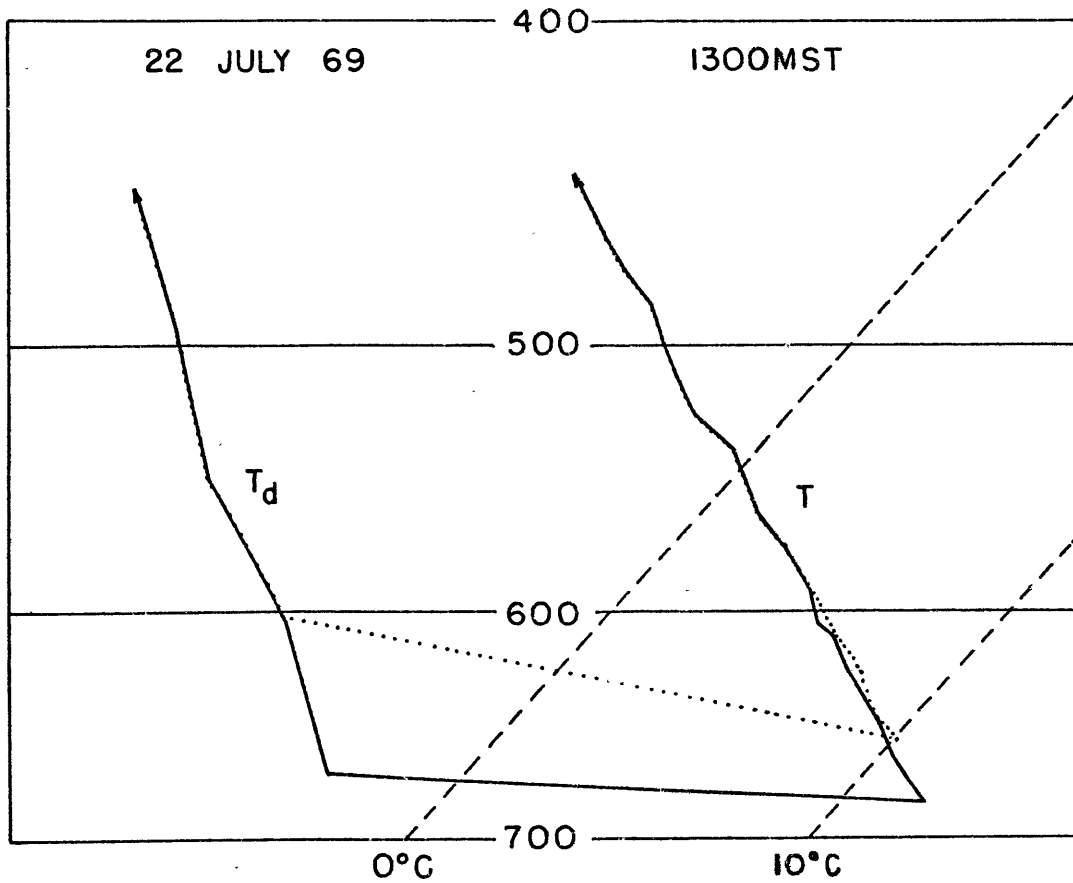


Figure 11. Two computer interpretations of sounding: solid lines have LCL as cloud base, dotted lines have CCL as cloud base.

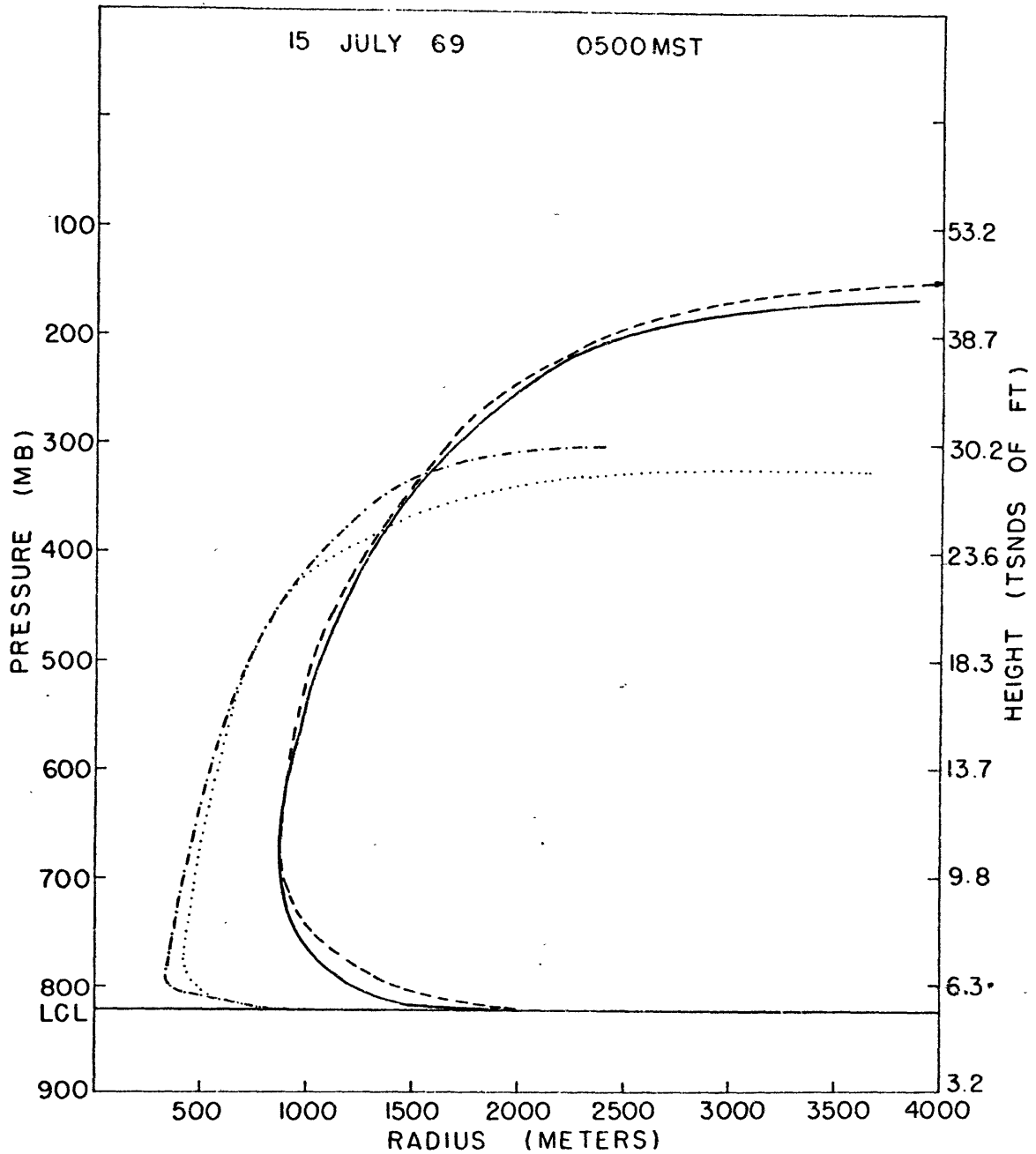


Figure 12. Dot-dash and dashed lines from sounding with even distribution of levels; dotted and solid lines from sounding with more lower levels; dotted and dot-dash lines initial conditions 1000,1; dashed and solid lines initial conditions 2000,2.

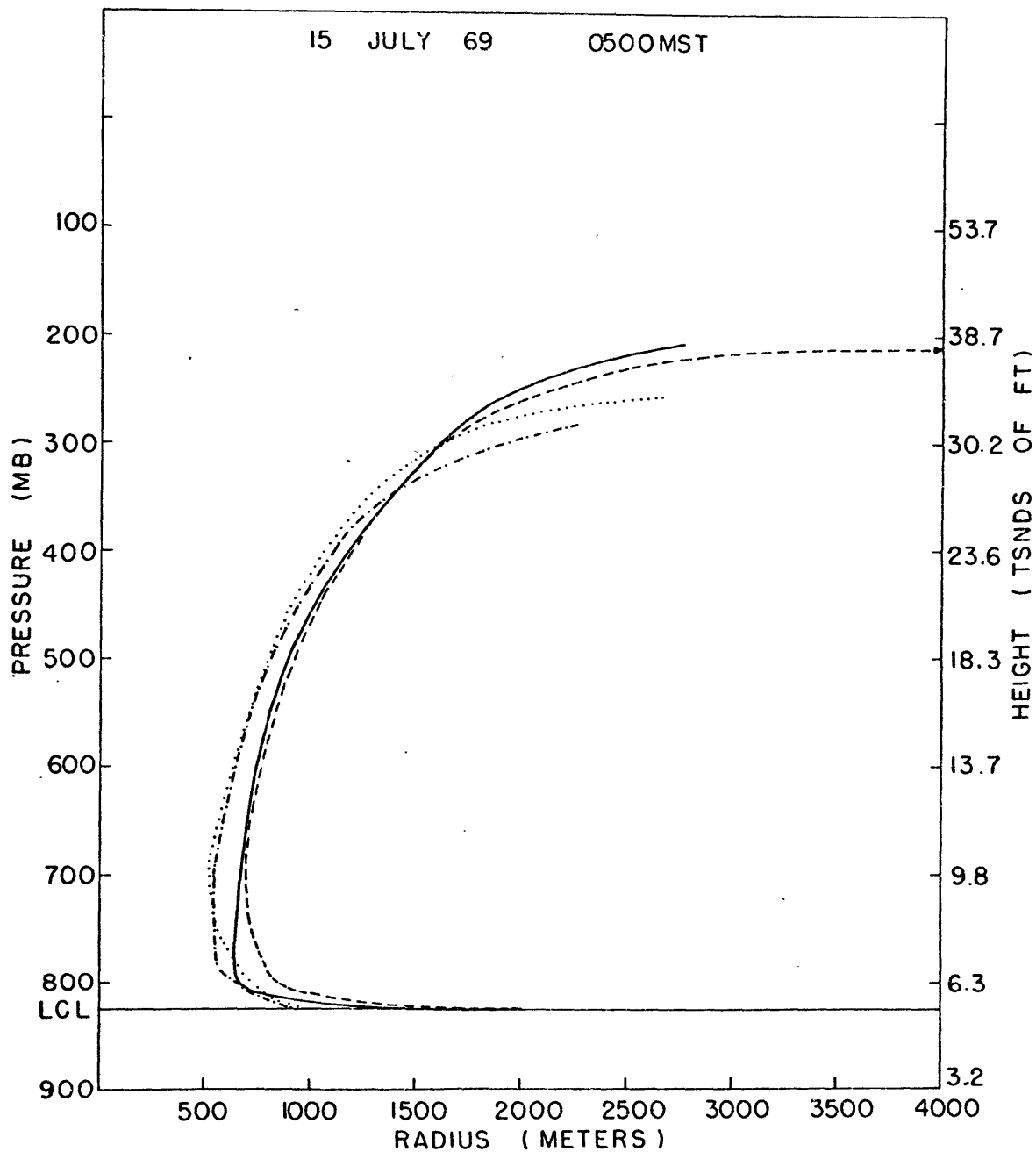


Figure 13. Dotted and solid lines from sounding with even distribution of levels; dot-dash and dashed lines from sounding with more lower levels; dotted and dot-dash lines initial conditions 1000,2; dashed and solid lines initial conditions 2000,1.

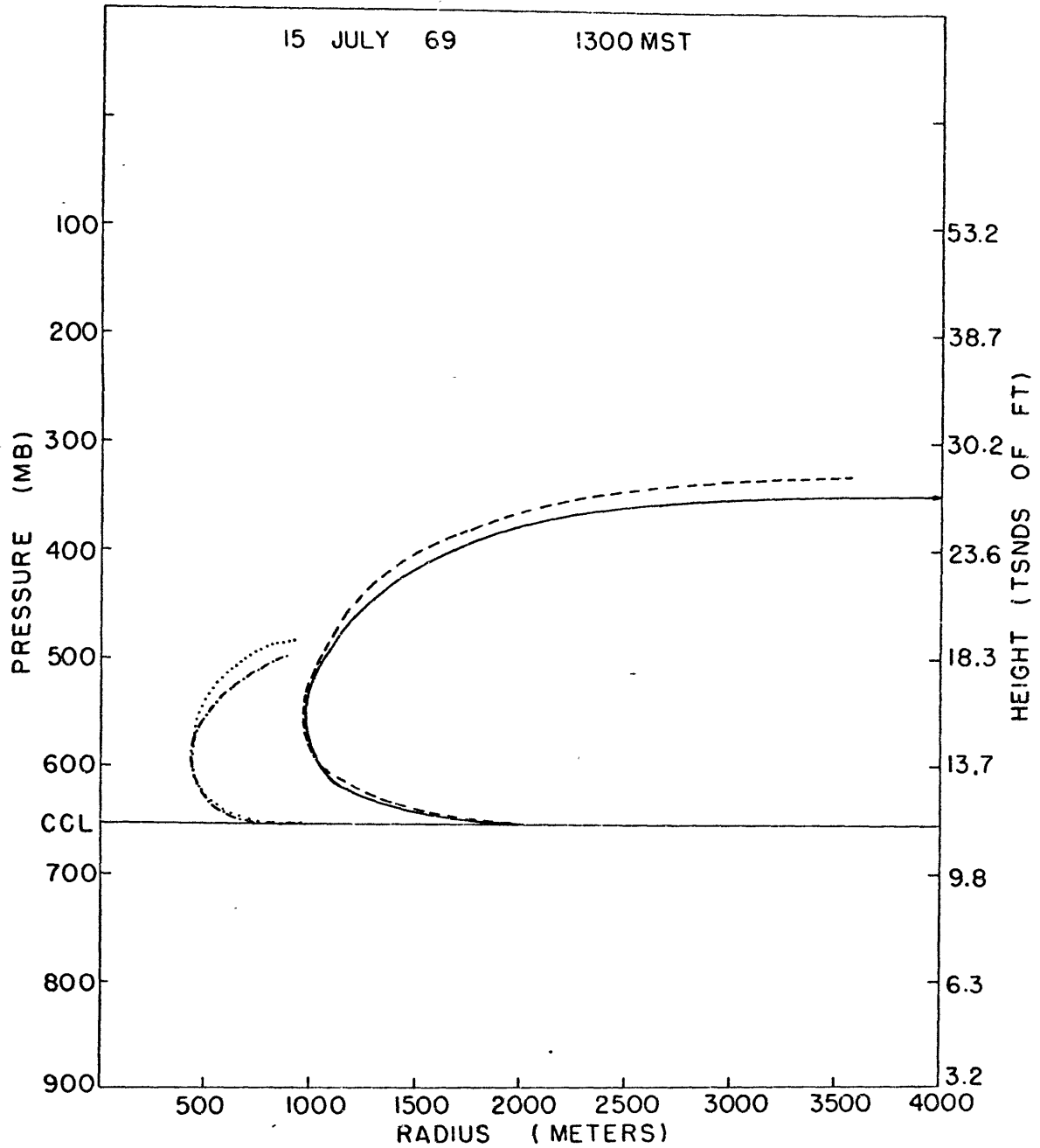


Figure 14. Dotted and dashed lines from sounding with even distribution of levels; dot-dash and solid lines from sounding with more lower levels; dotted and dot-dash lines initial conditions 1000,1; dashed and solid lines initial conditions 2000,2.

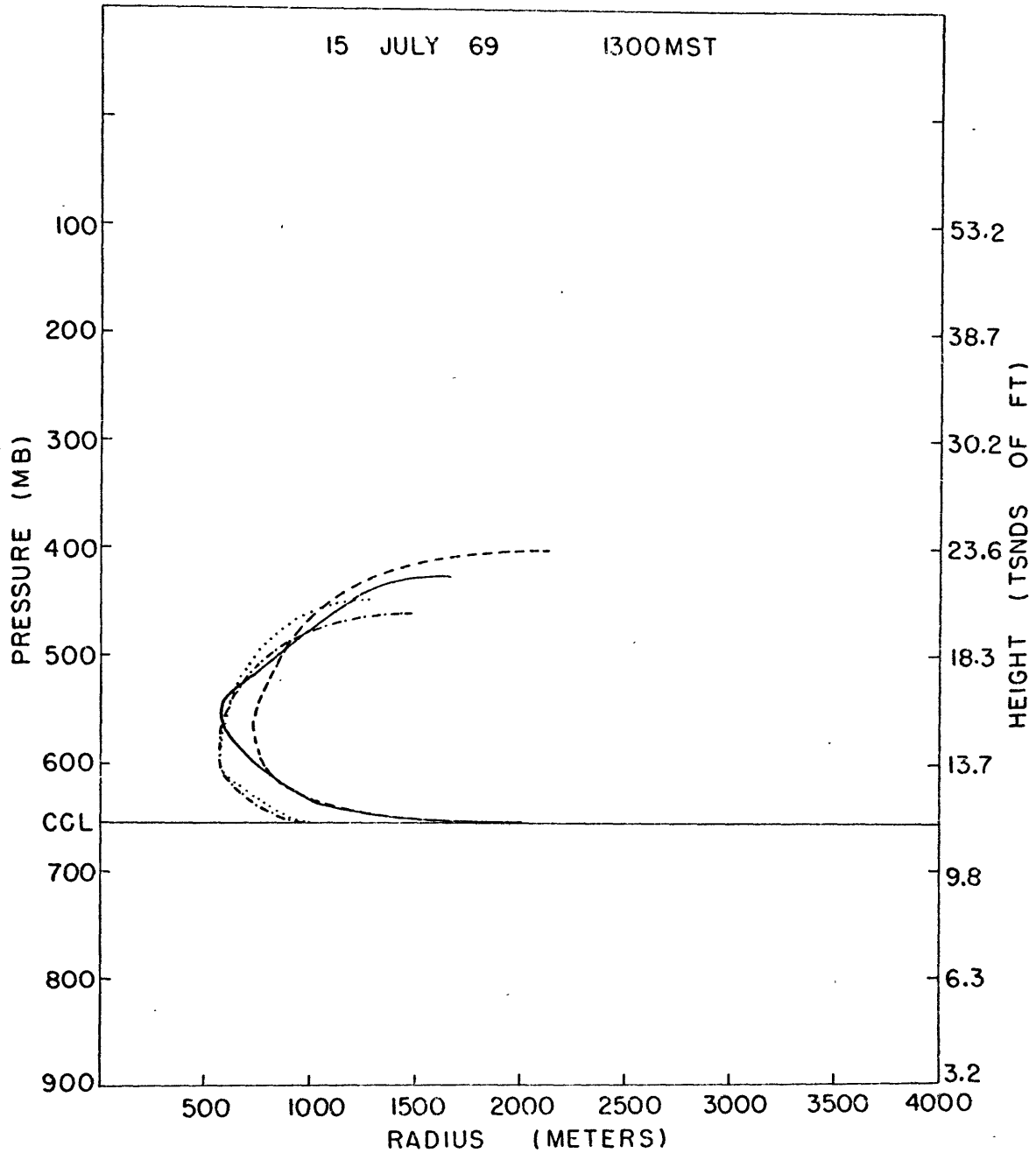


Figure 15. Dotted and dashed lines from sounding with even distribution of levels; dot-dash and solid lines from sounding with more lower levels; dotted and dot-dash lines initial conditions 1000,2; dashed and solid lines initial conditions 2000,1.

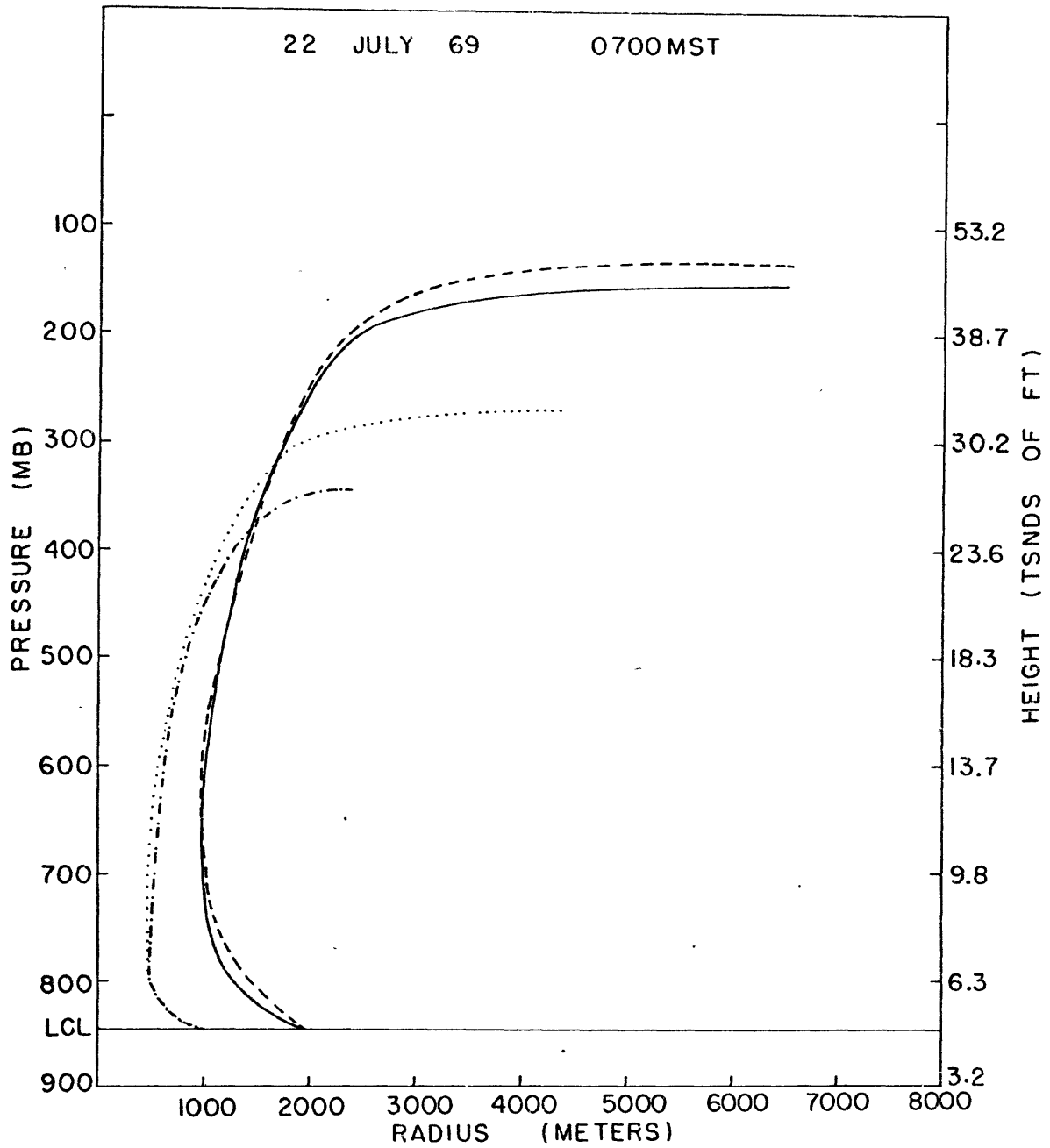


Figure 16. Dotted and dashed lines from sounding with even distribution of levels; dot-dash and solid lines from sounding with more lower levels; dotted and dot-dash lines initial conditions 1000,1; dashed and solid lines initial conditions 2000,2.

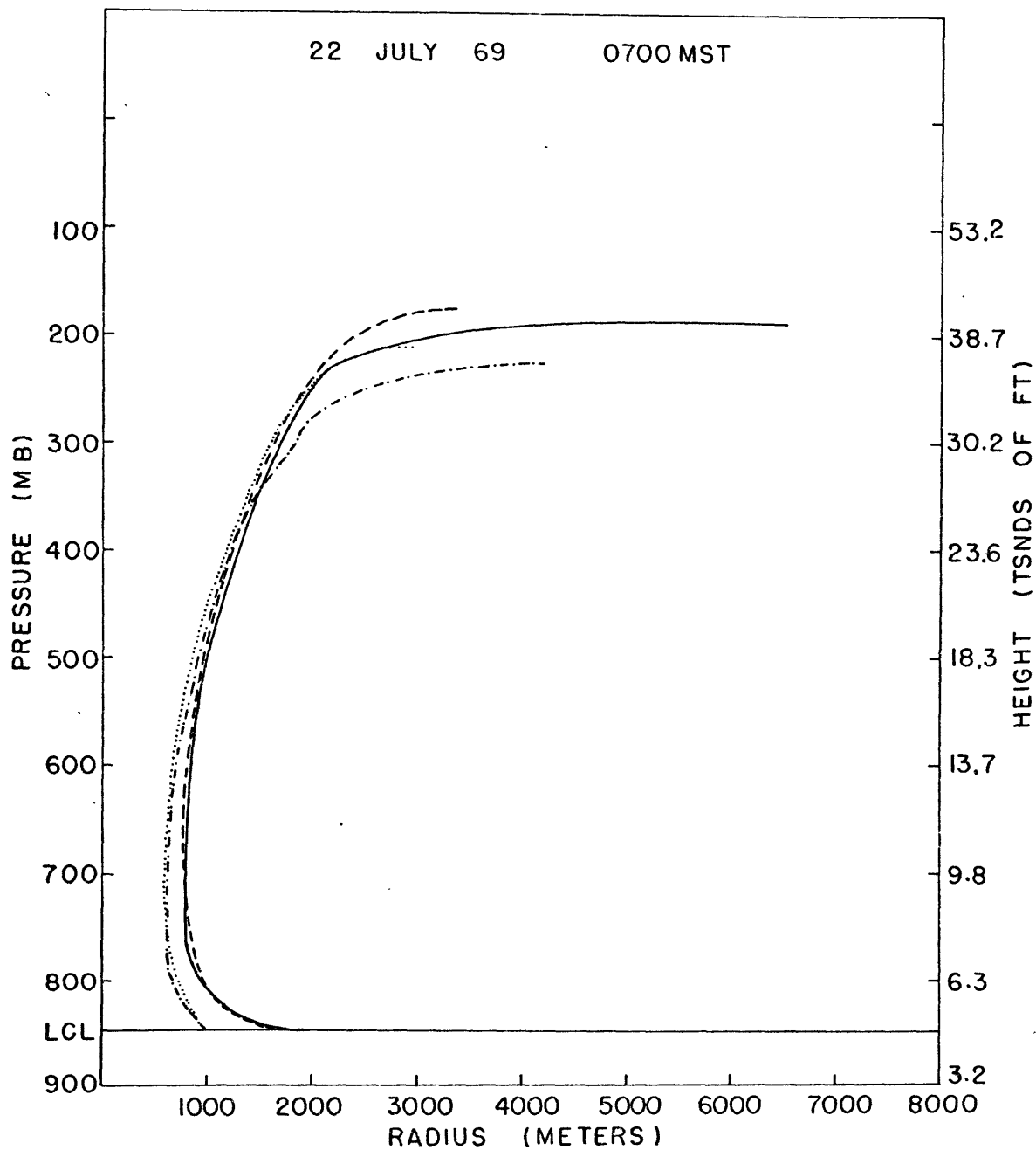


Figure 17. Dotted and dashed lines from sounding with even distribution of levels; dot-dash and solid lines from sounding with more lower levels; dotted and dot-dash lines initial conditions 1000,2; dashed and solid lines initial conditions 2000,1.

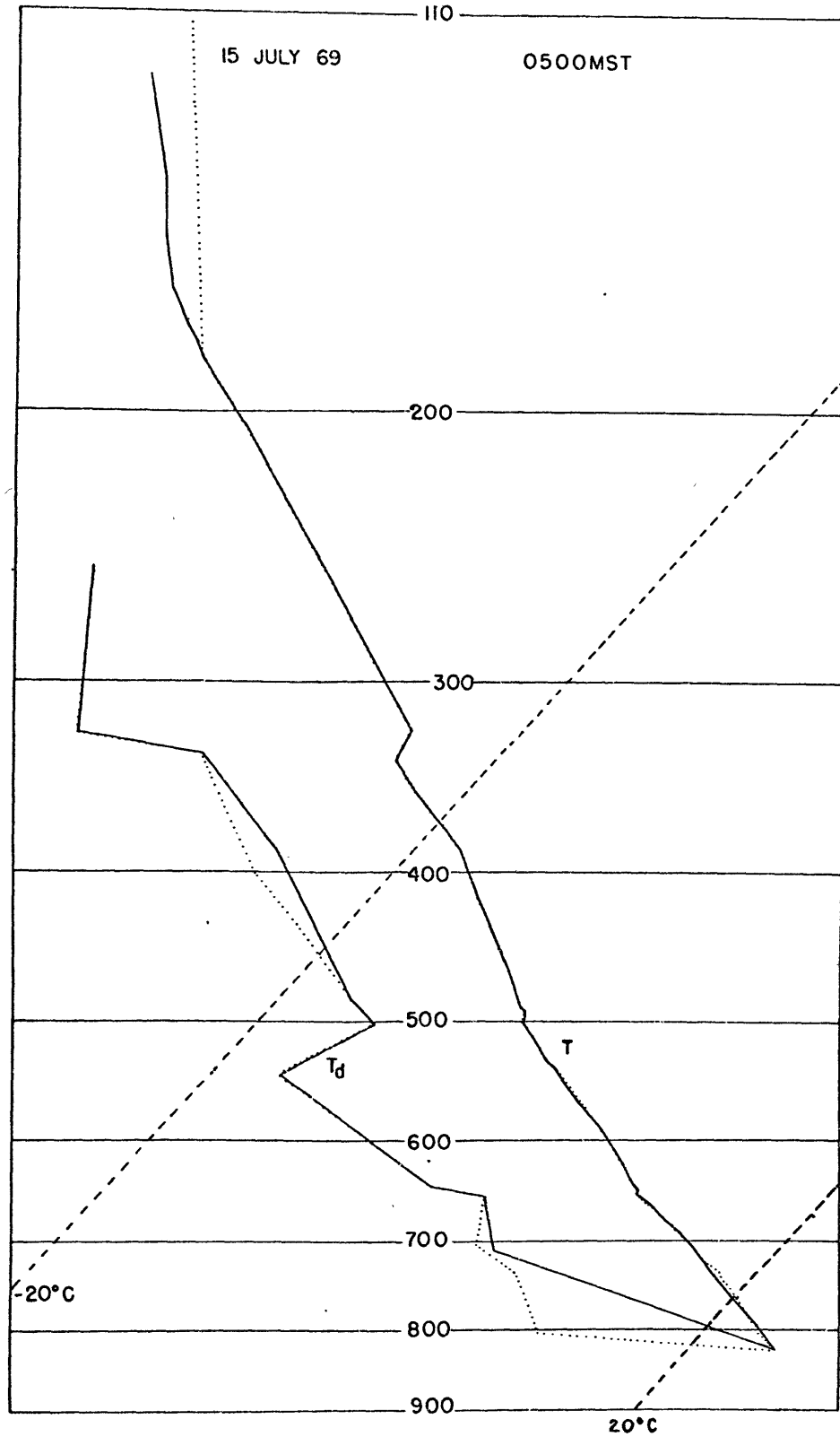


Figure 18. Solid lines are interpretation of sounding with even distribution of input levels; dotted lines are interpretation of sounding with more lower input levels.

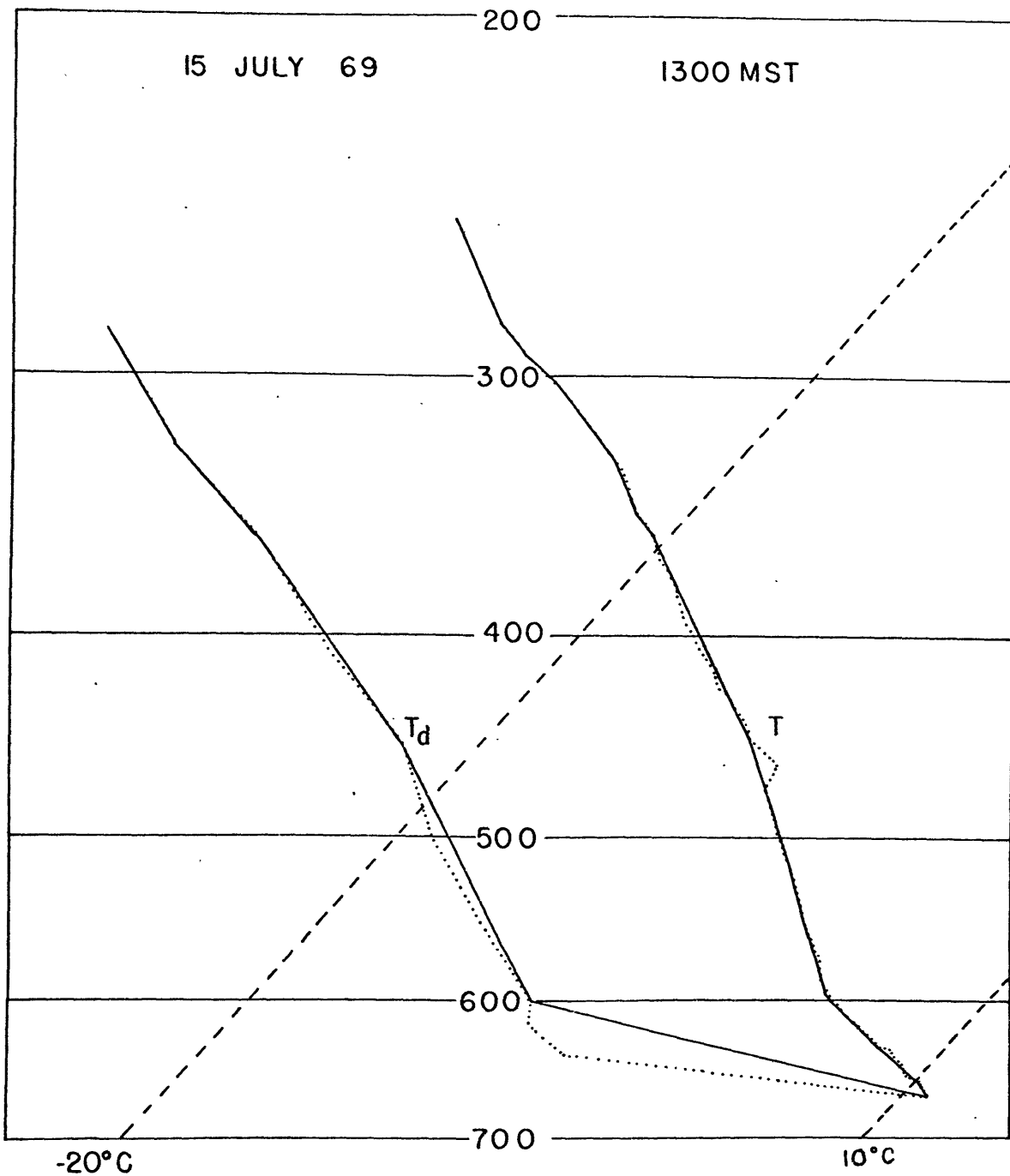


Figure 19. Solid lines are interpretation of sounding with even distribution of input levels; dotted lines are interpretation of sounding with more lower input levels.

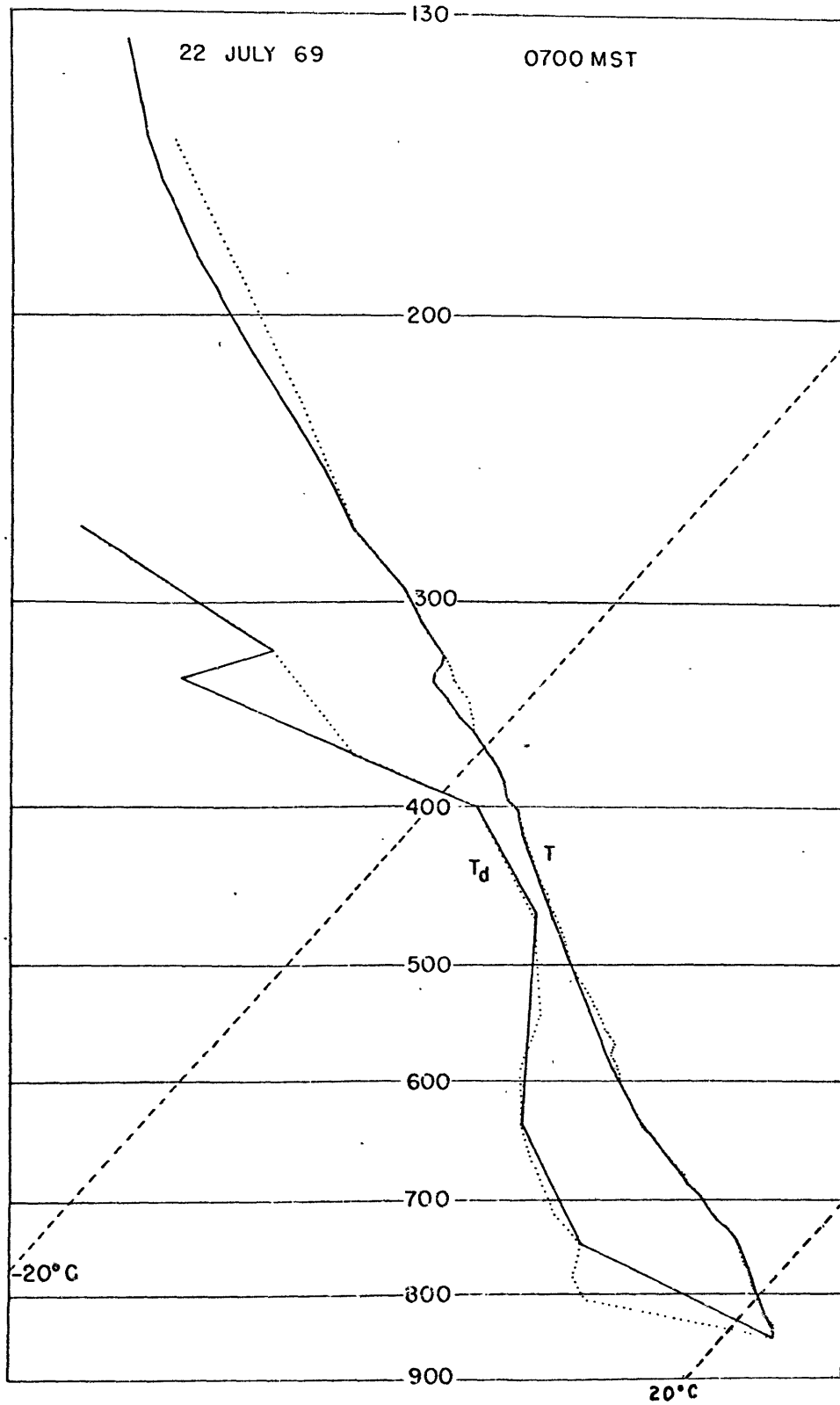


Figure 20. Solid lines are interpretation of sounding with even distribution of input levels; dotted lines are interpretation of sounding with more lower input levels.

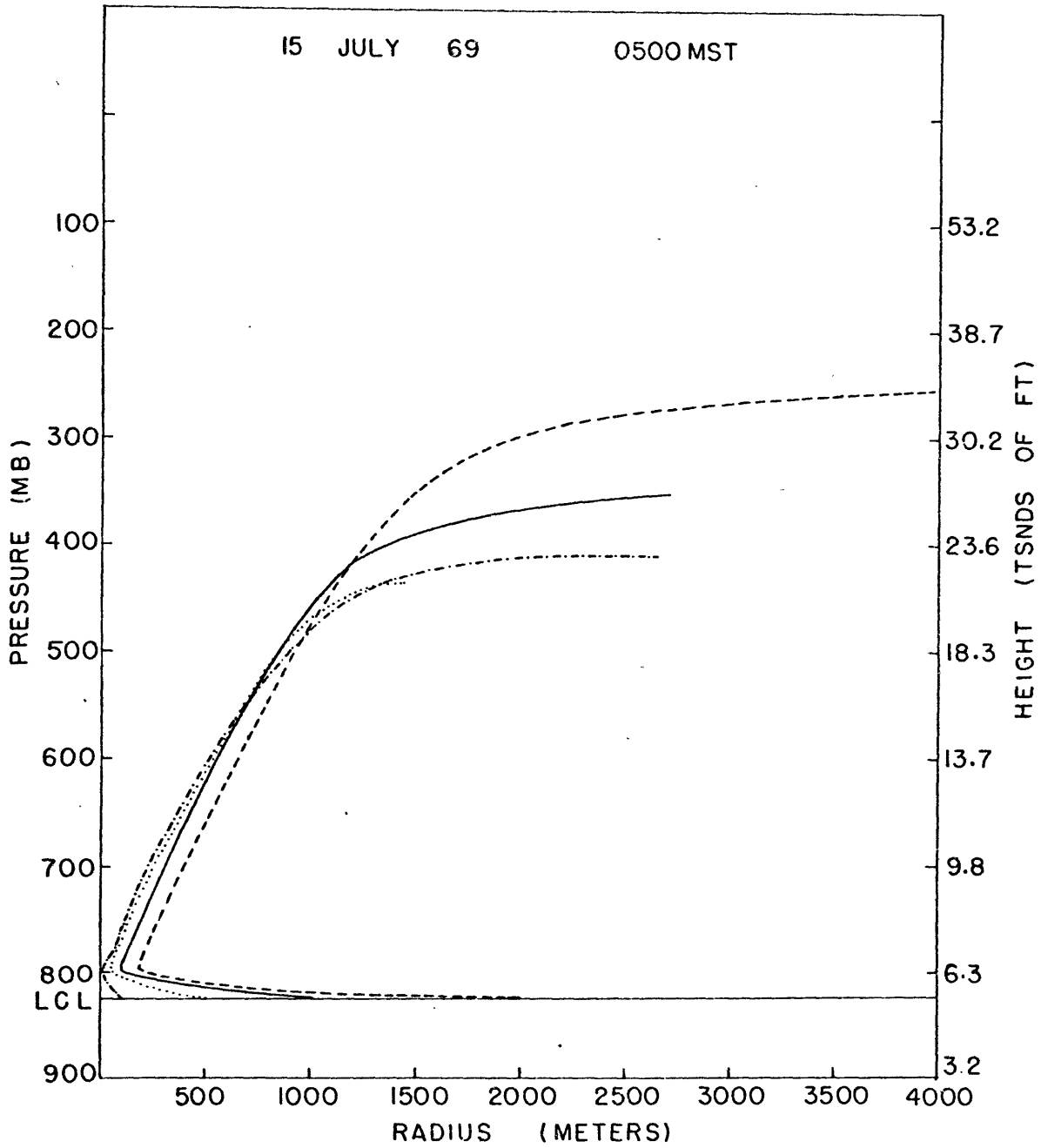


Figure 21. Initial conditions: dot-dash line 100,0.5; dotted line 500,0.5; solid line 1000,0.5; dashed line 2000,0.5.

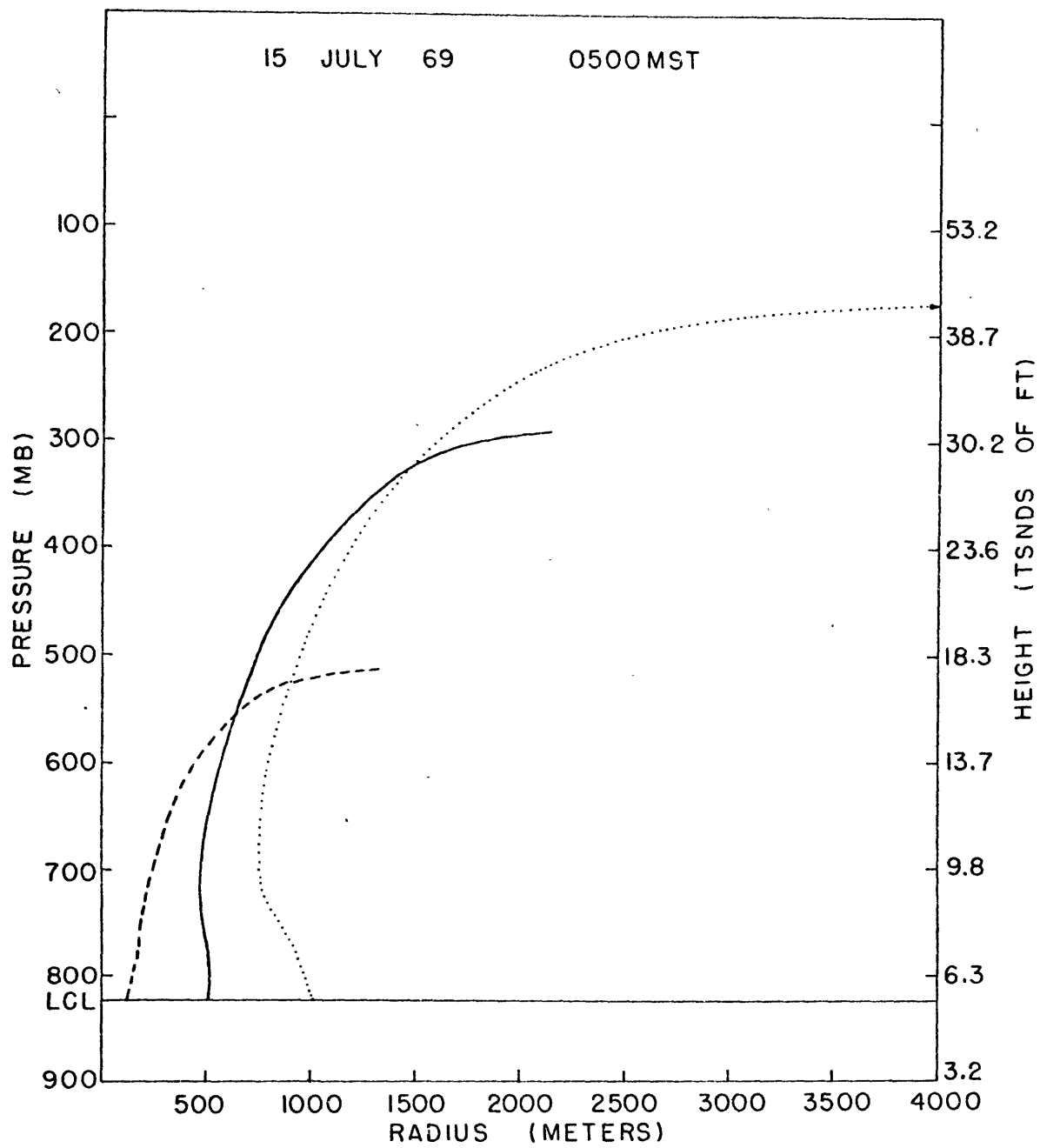


Figure 22. Initial conditions: dashed line 100,5; solid line 500,5; dotted line 1000,5.

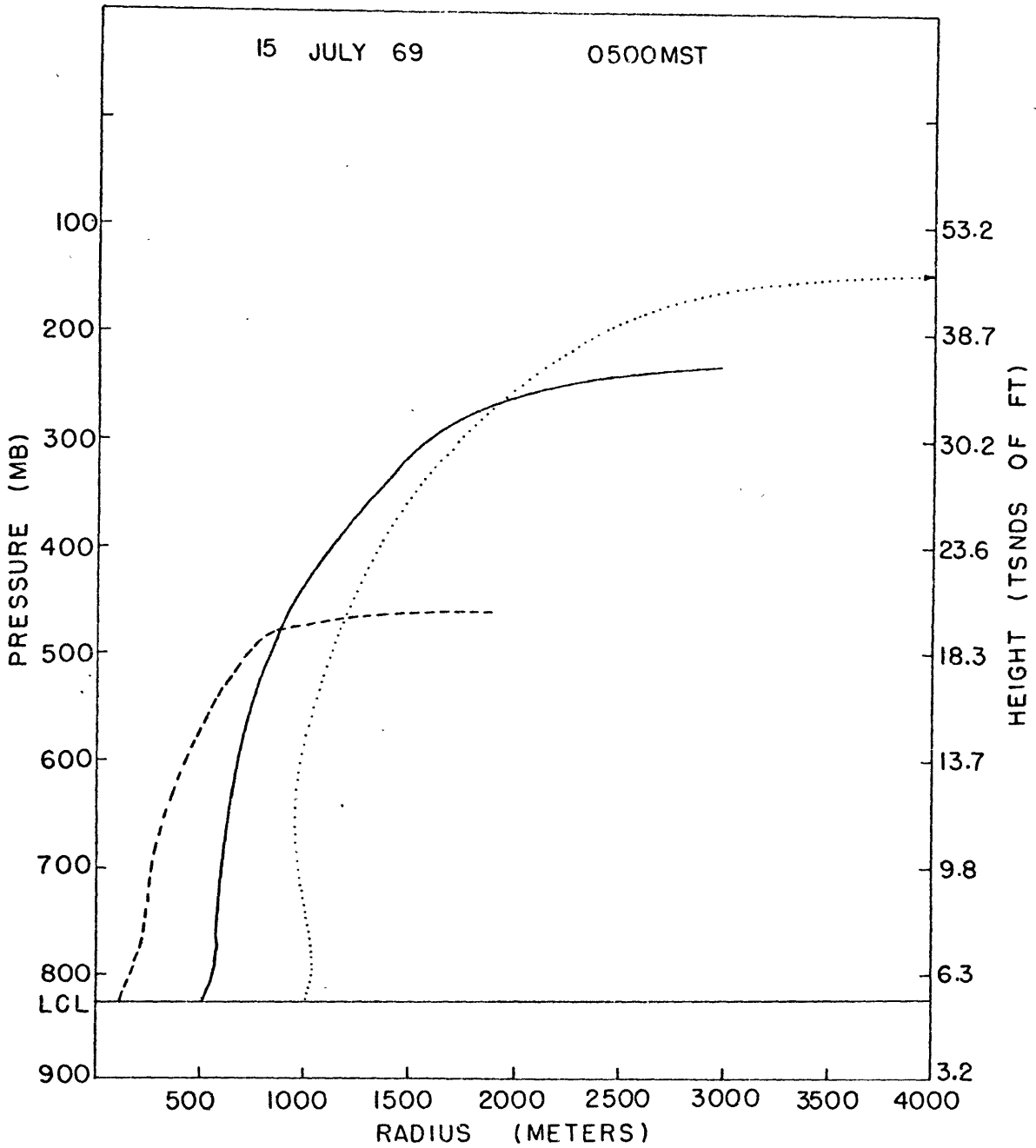


Figure 23. Initial conditions: dashed line 100,10; solid line 500,10; dotted line 1000,10.

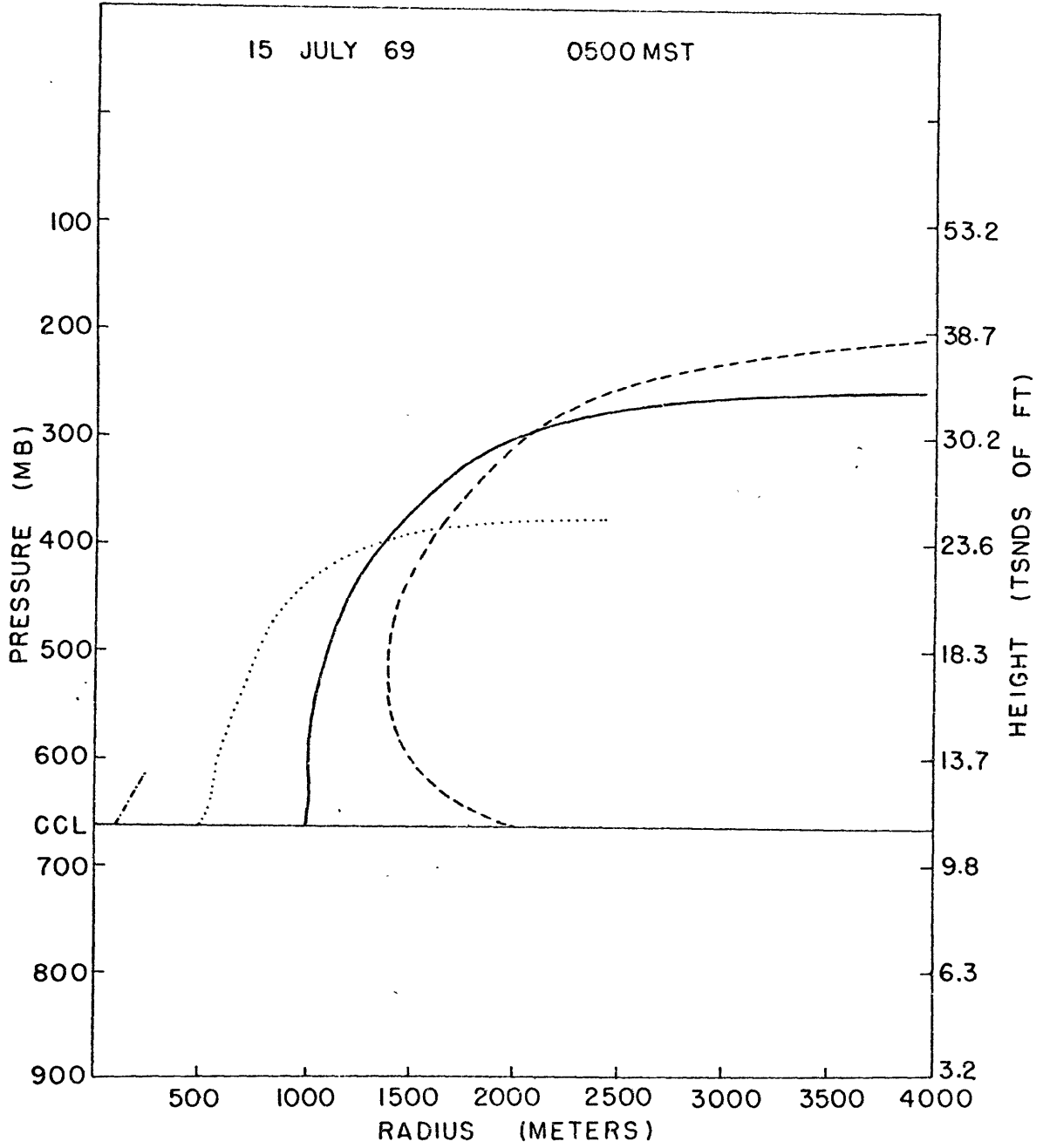


Figure 24. Initial conditions: dot-dash line 100,10; dotted line 500,10; solid line 1000,10; dashed line 2000,5.

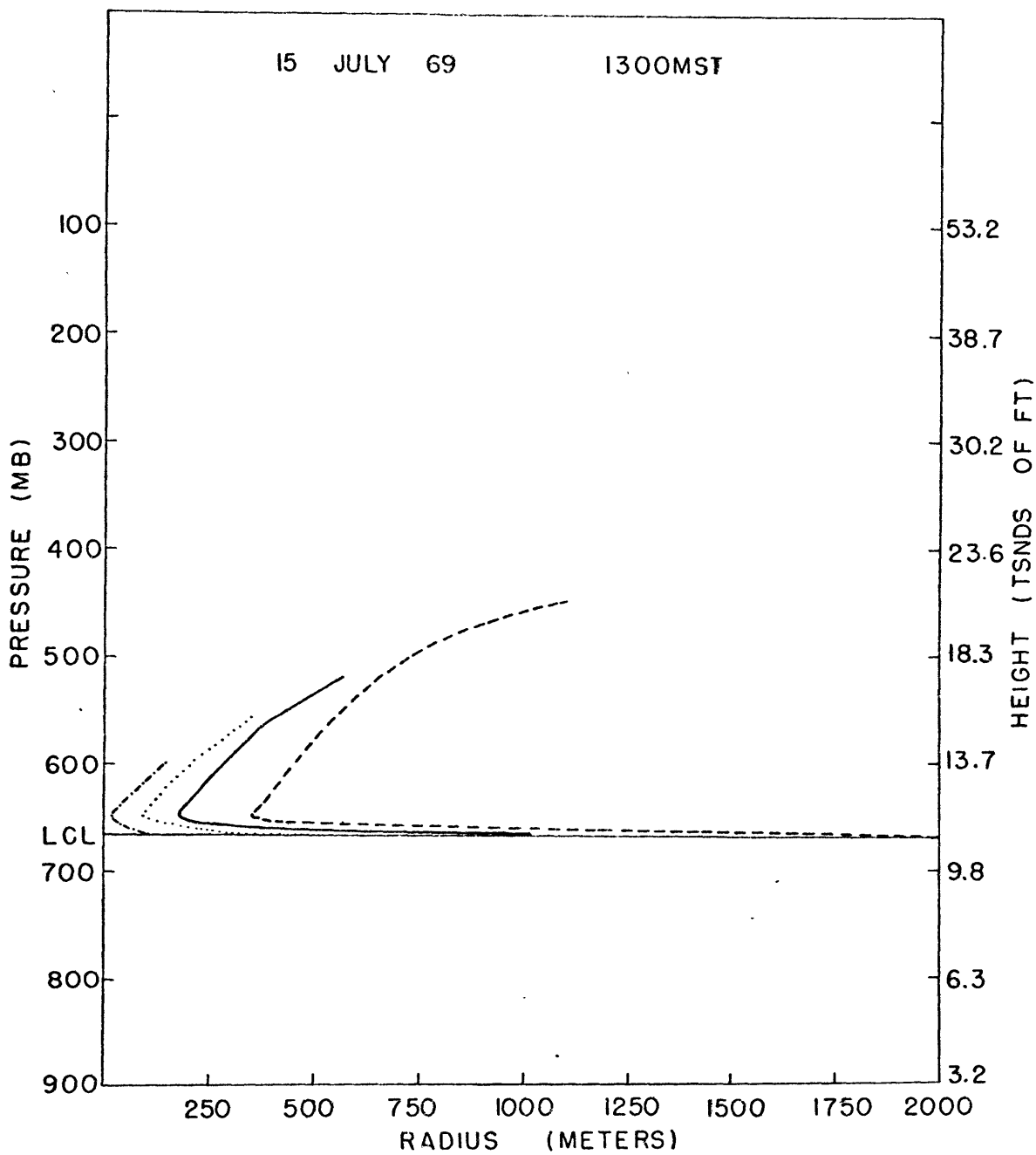


Figure 25. Initial conditions: dot-dash line 100,0.5; dotted line 500,0.5; solid line 1000,0.5; dashed line 2000,0.5.

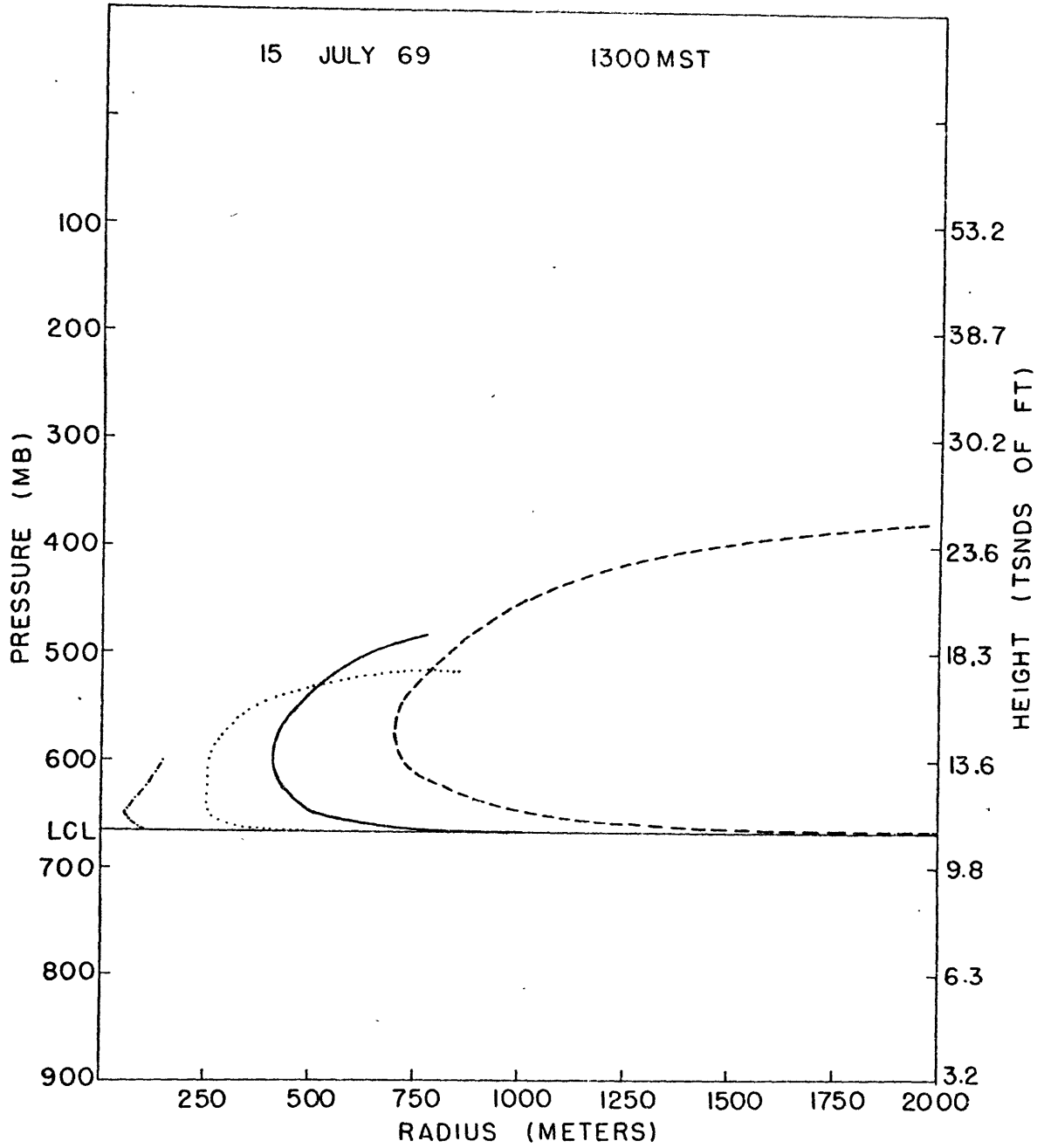


Figure 26. Initial conditions: dot-dash line 100,1; dotted line 500,1; solid line 1000,1; dashed line 2000,1.

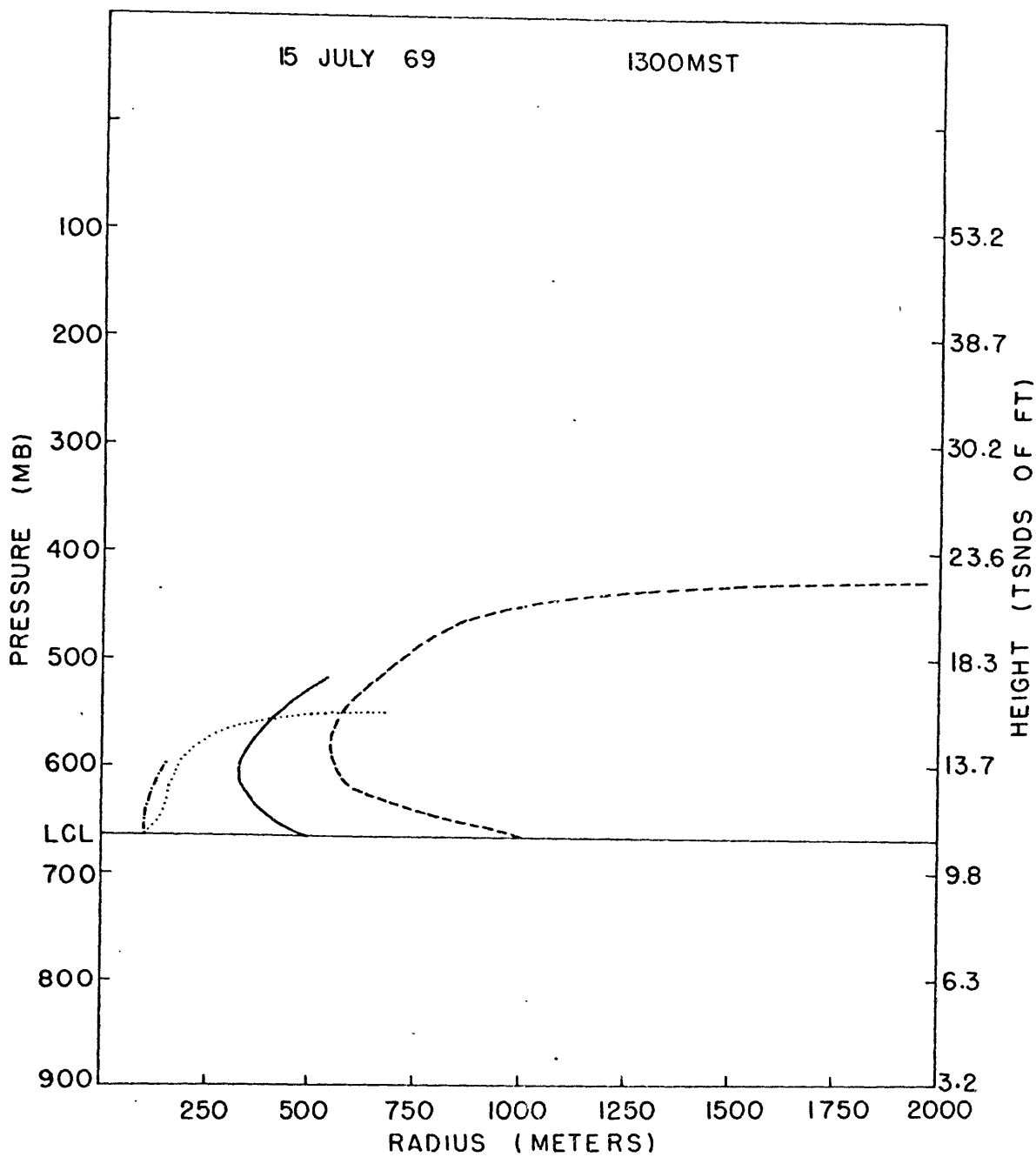


Figure 27. Initial conditions: dot-dash line 100,2; dotted line 100,5; solid line 500,2; dashed line 1000,2.

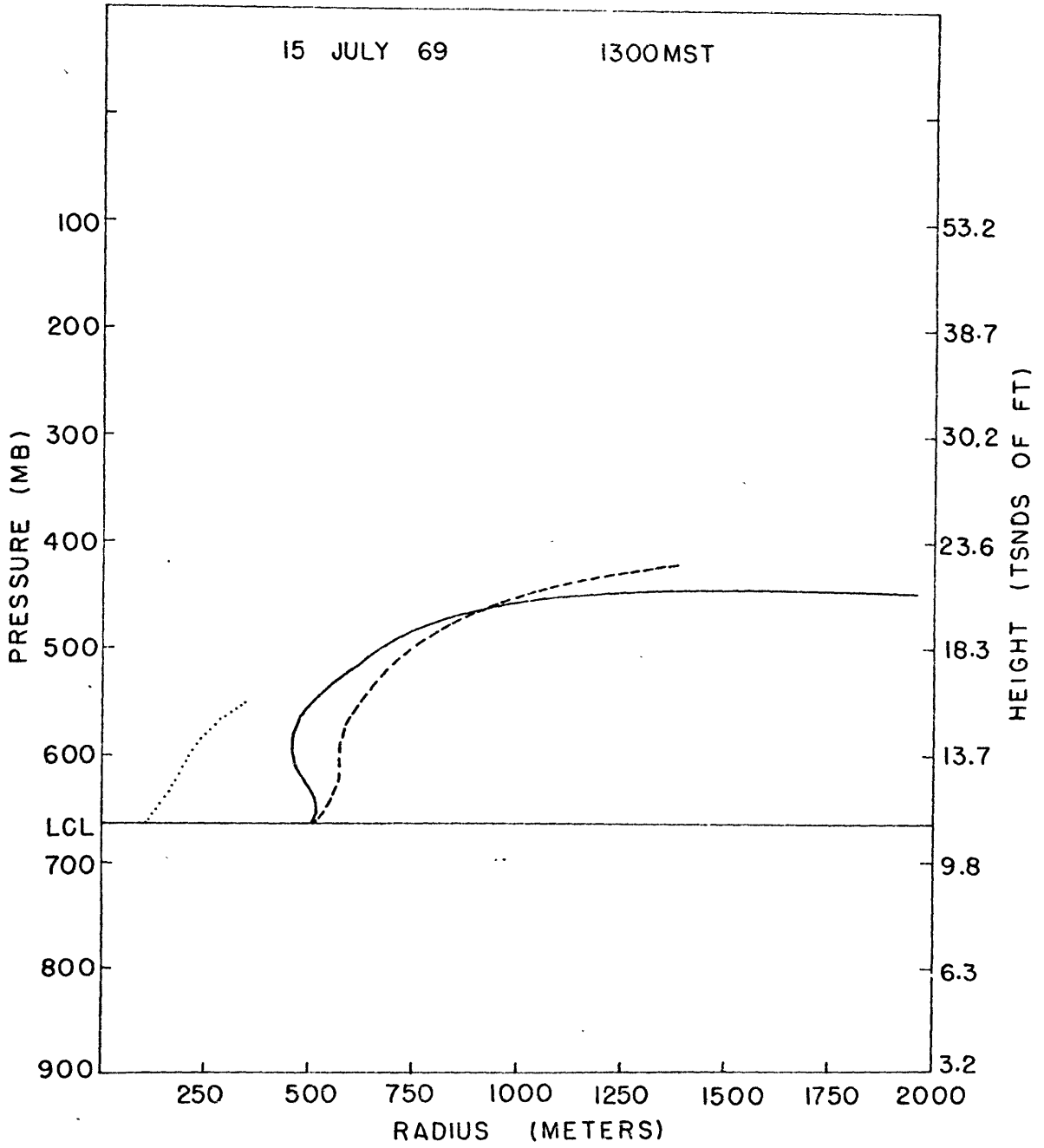


Figure 28. Initial conditions: dotted line 100,10; solid line 500,5; dashed line 500,10.

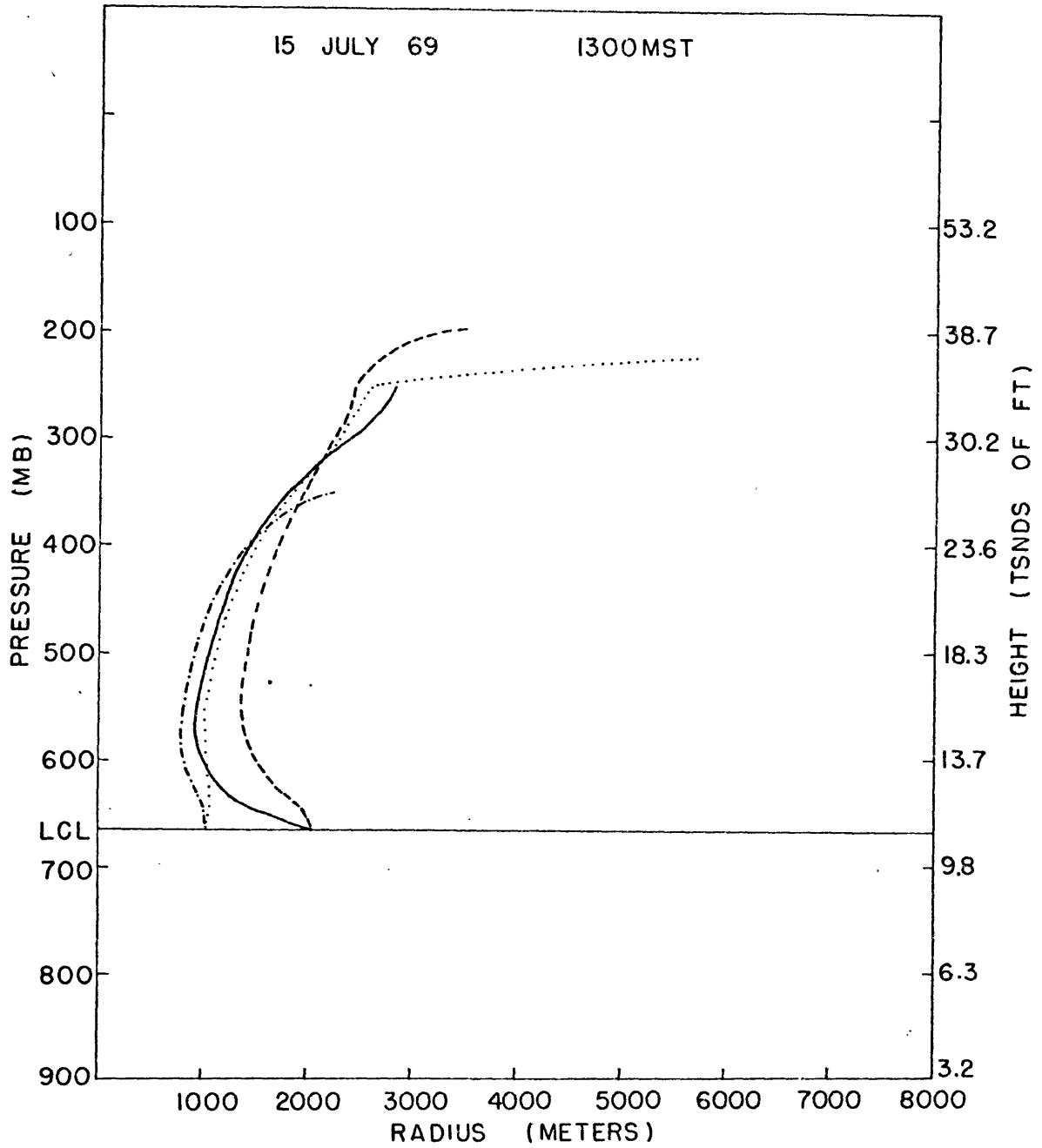


Figure 29. Initial conditions: dot-dash line 1000,5; dotted line 1000,10; solid line 2000,2; dashed line 2000,5.

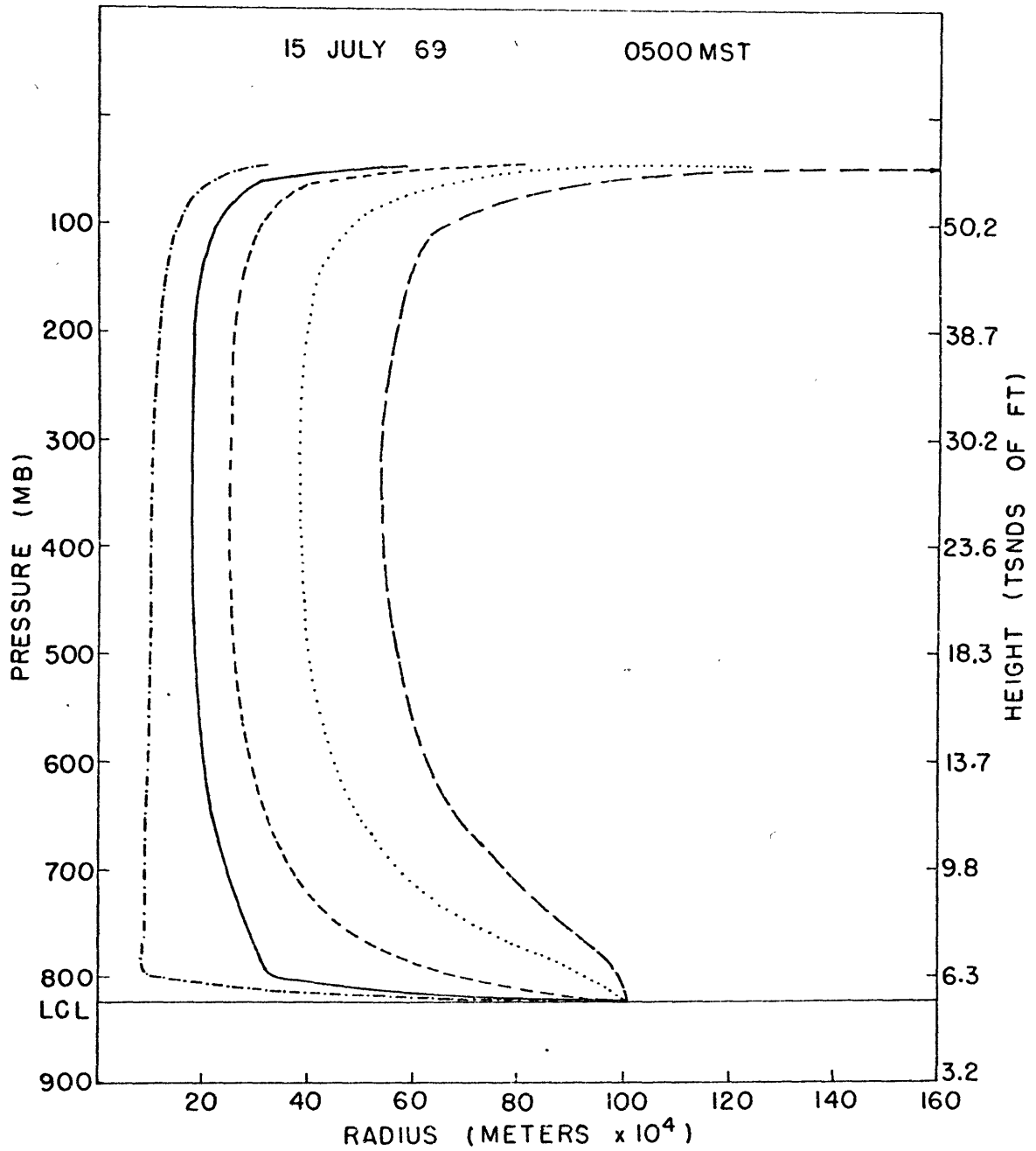


Figure 30. Initial radius 1,000,000; initial vertical velocities: dot-dash line 0.5; solid line 1; short-dashed line 2; dotted line 5; long-dashed line 10.

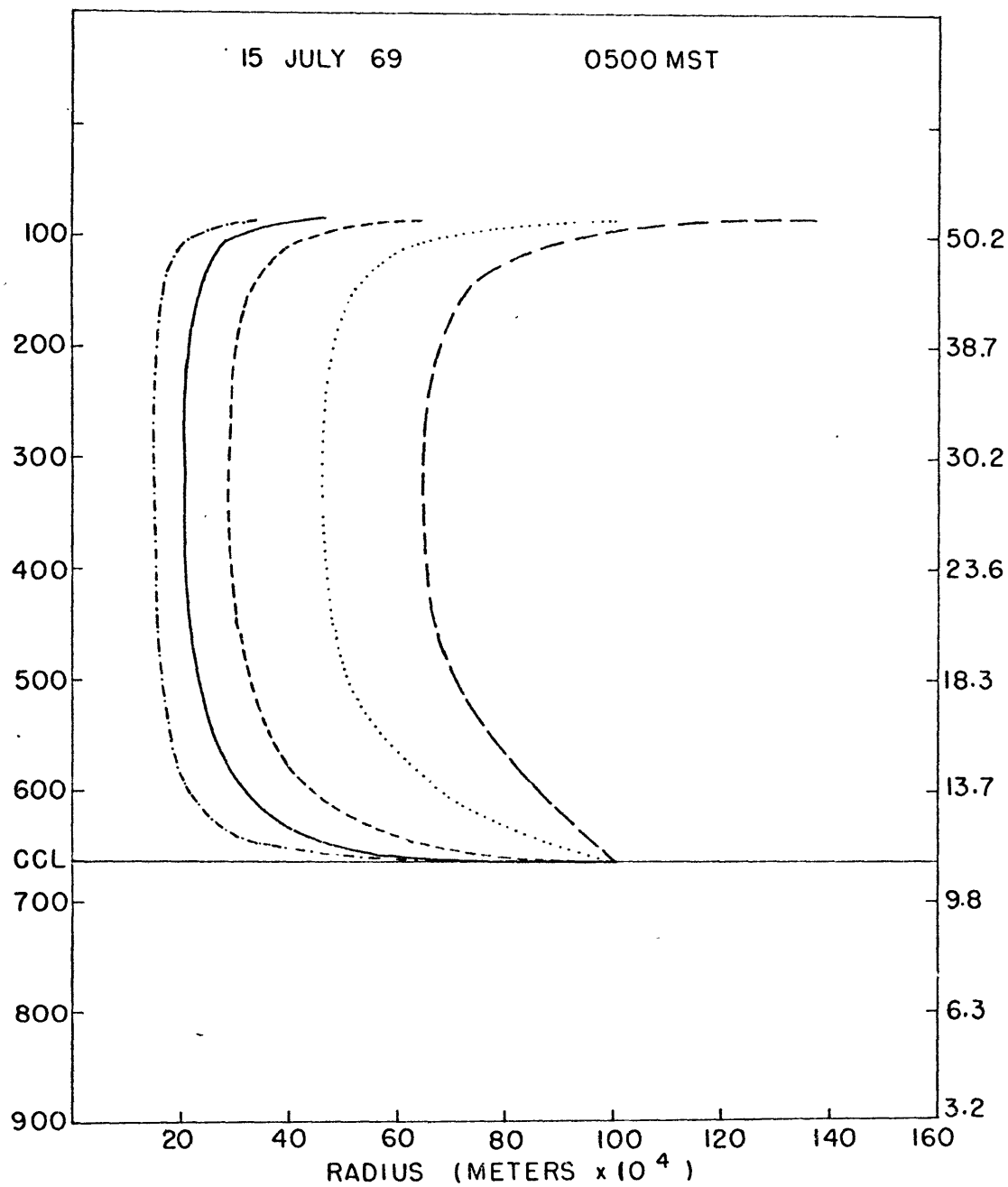


Figure 31. Initial radius 1,000,000; initial vertical velocities: dot-dash line 0.5; solid line 1; short-dashed line 2; dotted line 5; long-dashed line 10.

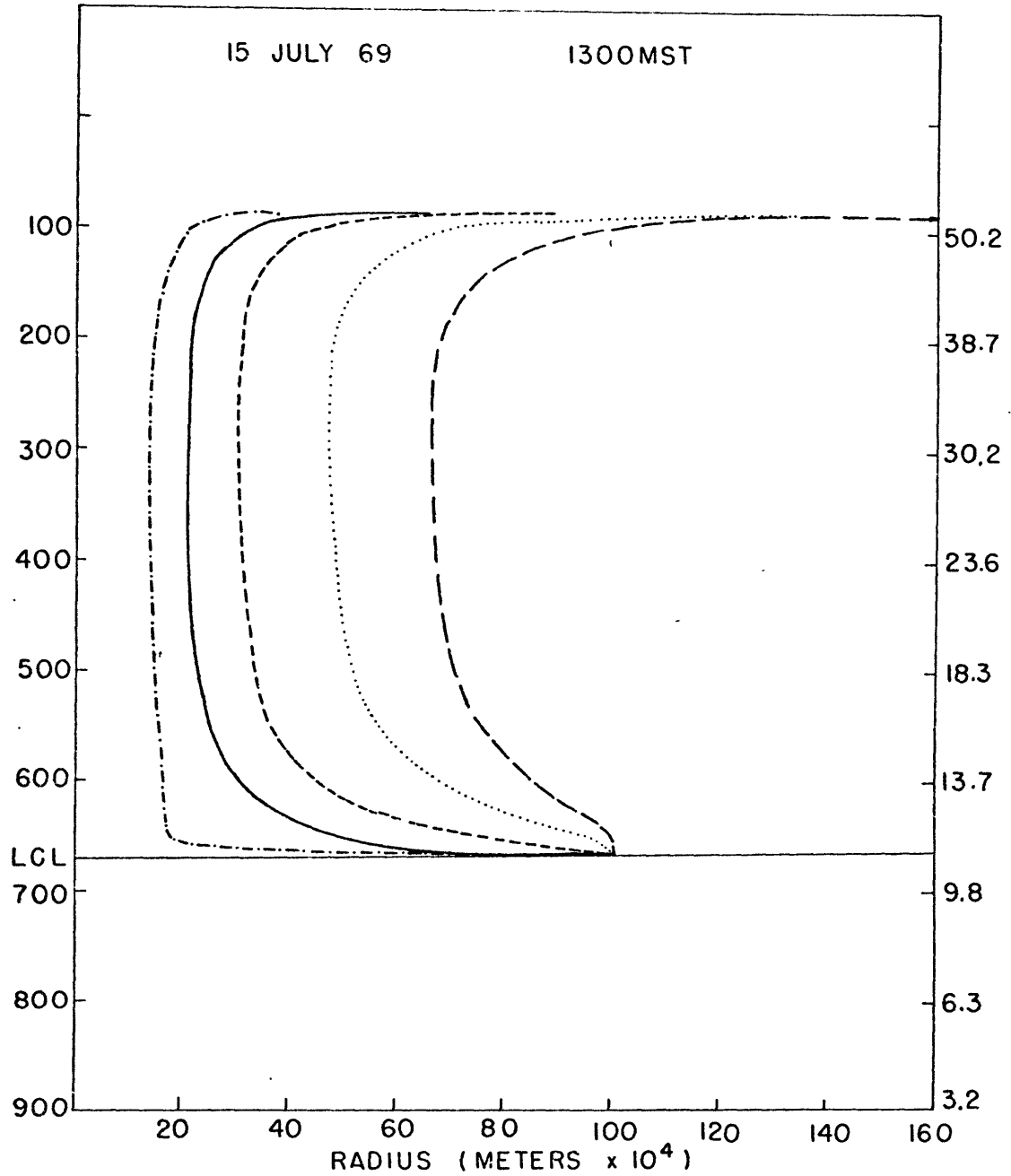


Figure 32. Initial radius 1,000,000; initial vertical velocities: dot-dash line 0.5; solid line 1; short-dashed line 2; dotted line 5; long-dashed line 10.

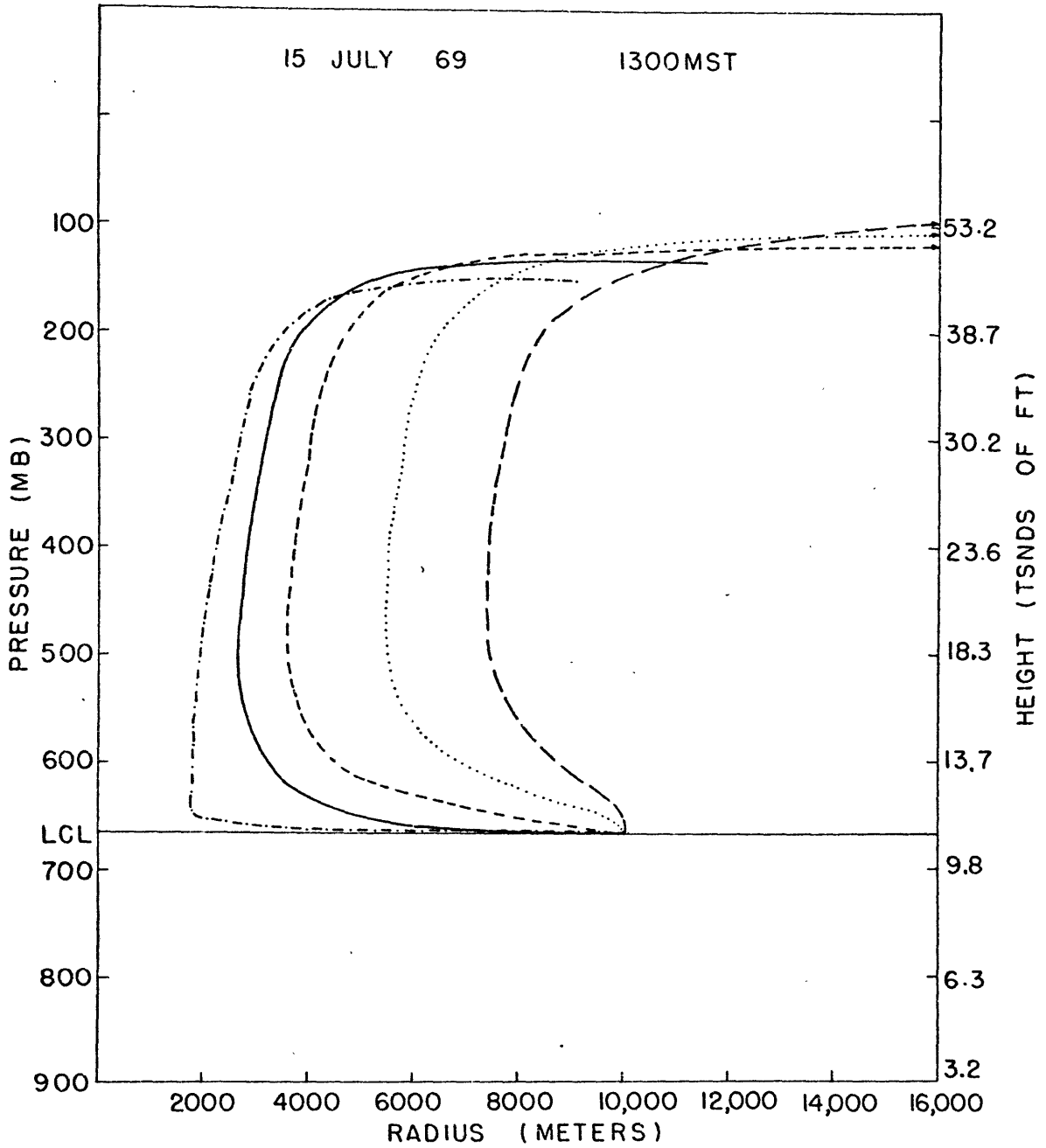


Figure 33. Initial radius 10,000; initial vertical velocities: dot-dash line 0.5; solid line 1; short-dashed line 2; dotted line 5; long-dashed line 10.

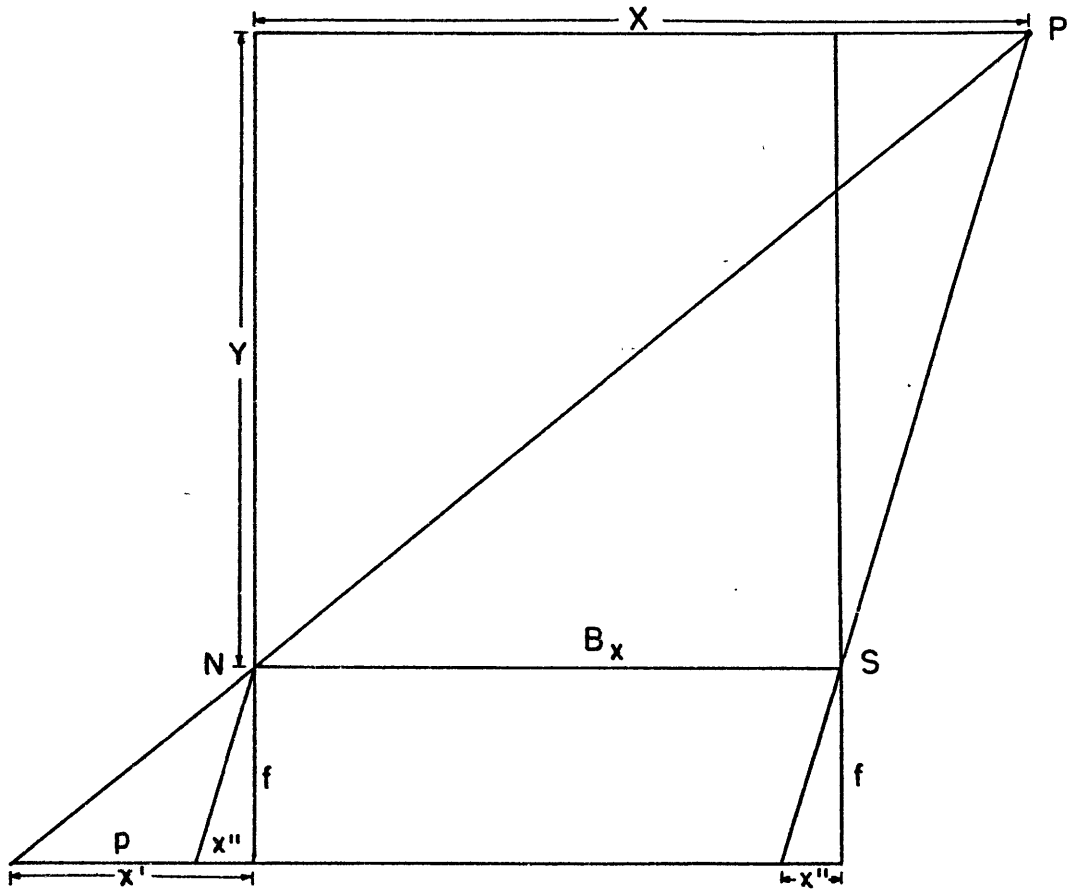


Figure 34.

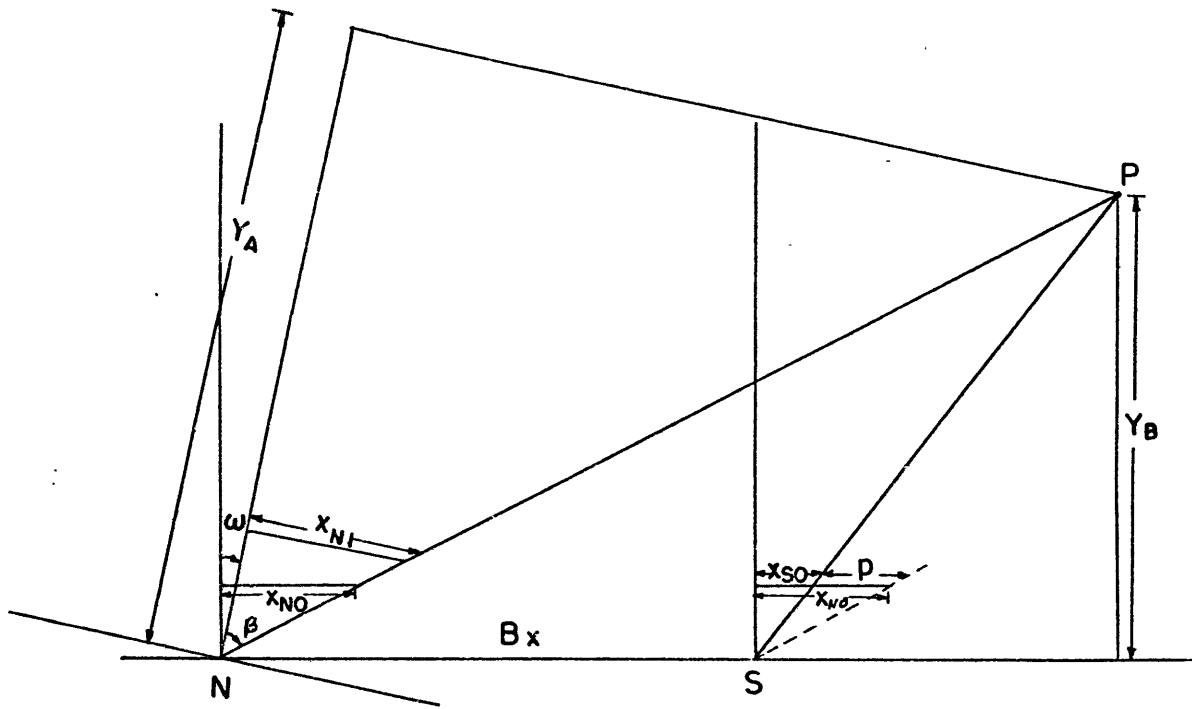


Figure 35.

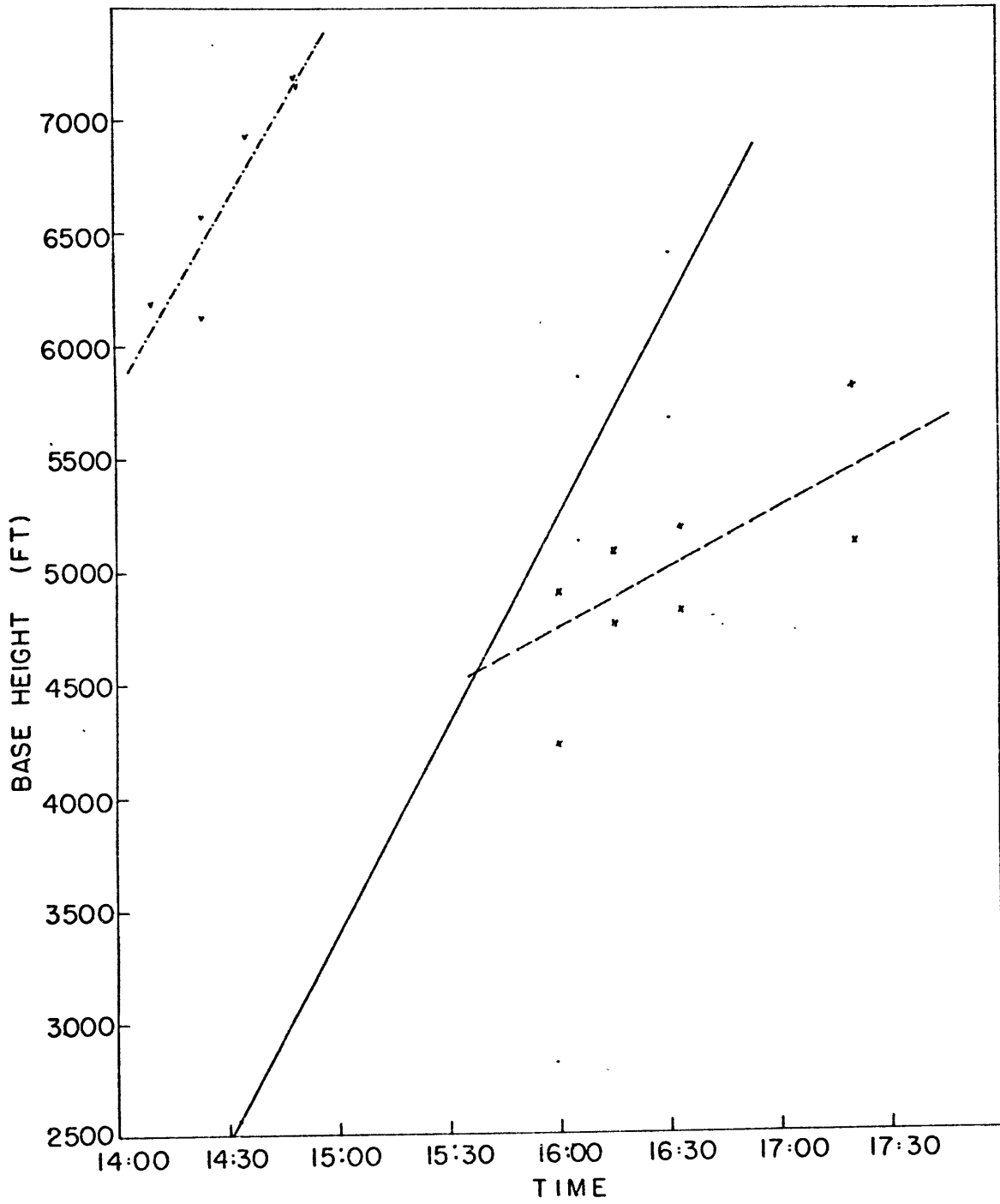


Figure 36.

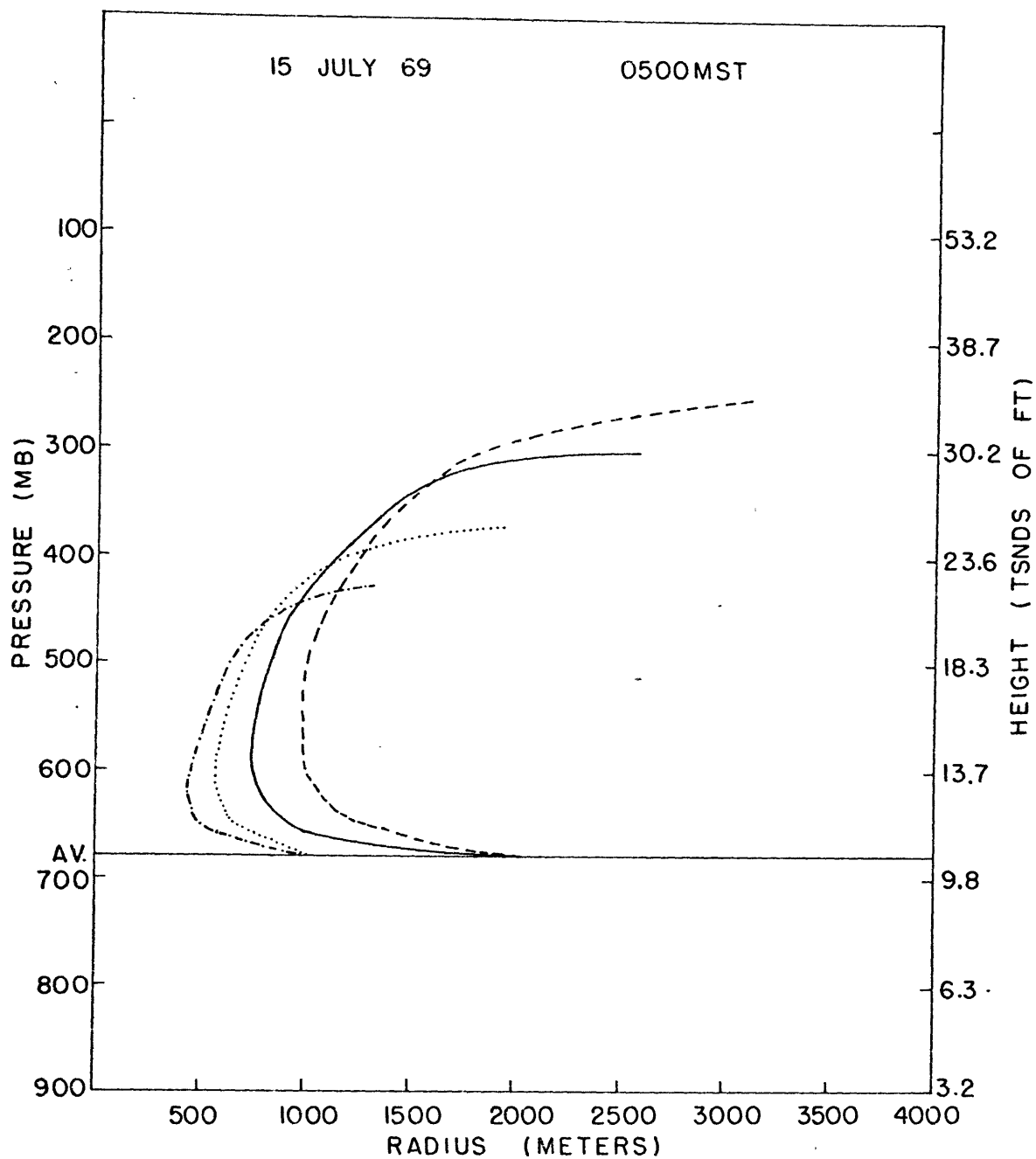


Figure 37. Initial conditions: dot-dash line 1000,1; dotted line 1000,2; solid line 2000,1; dashed line 2000,2.

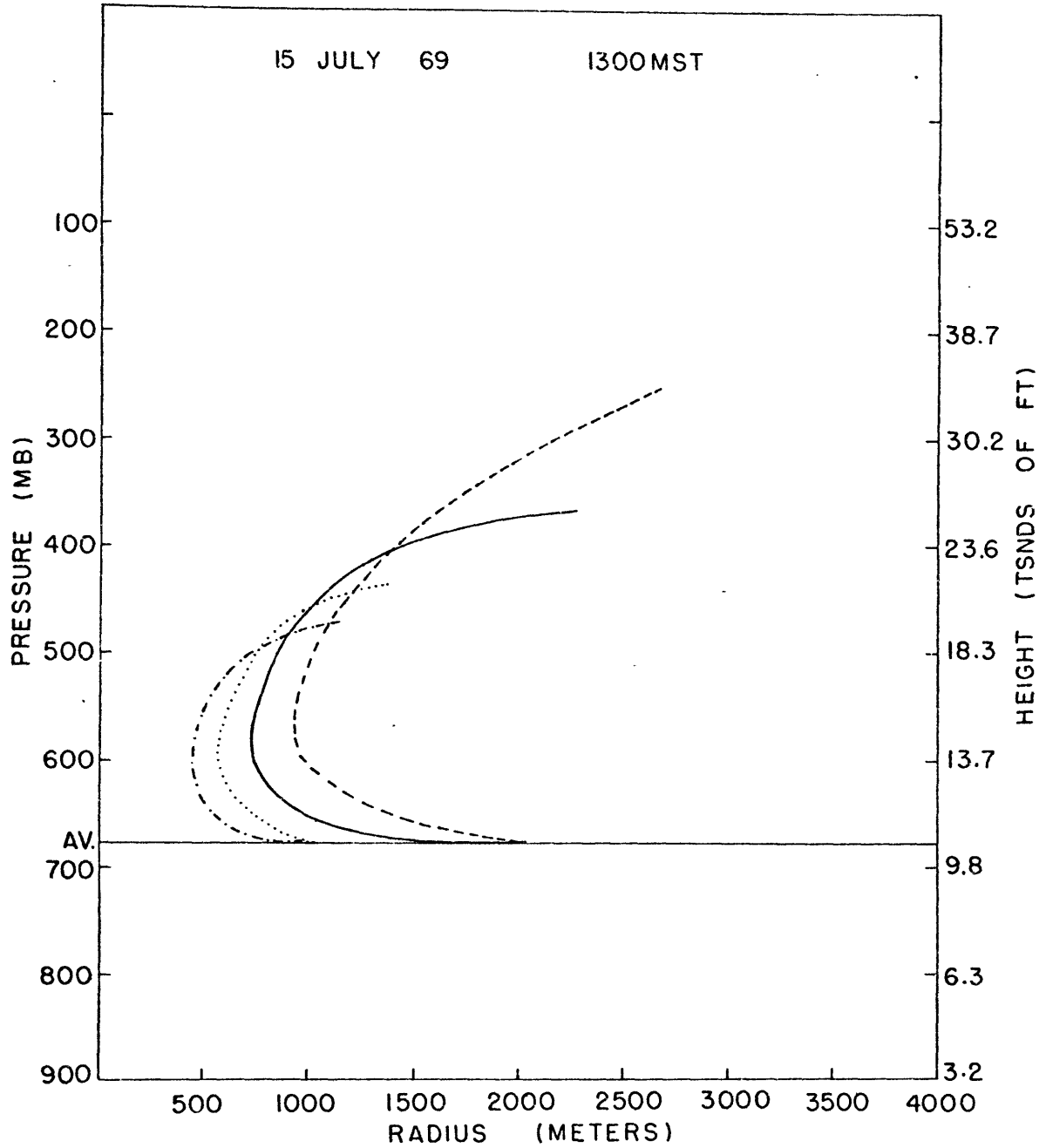


Figure 38. Initial conditions: dot-dash line 1000,1; dotted line 1000,2; solid line 2000,1; dashed line 2000,2.

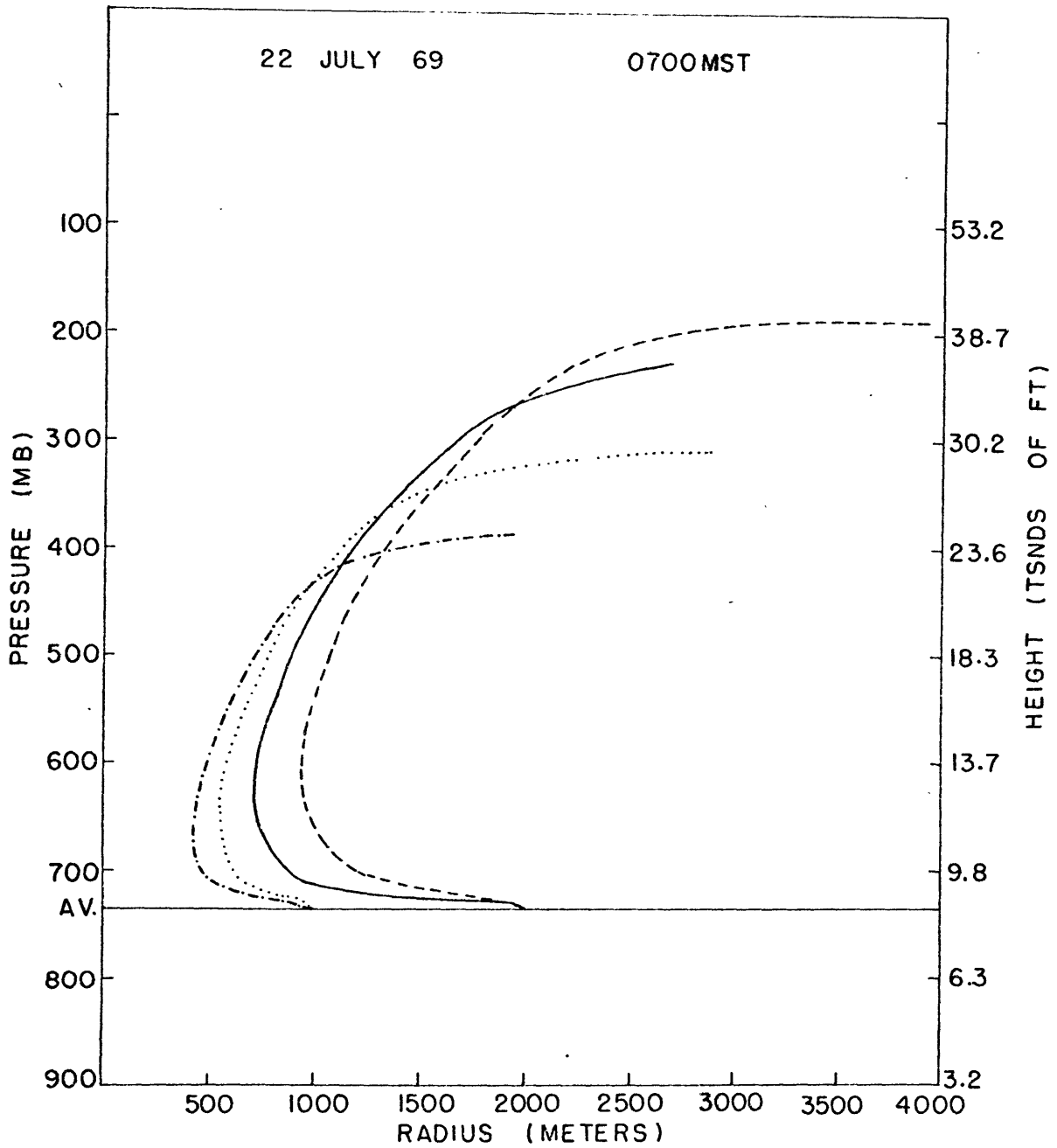


Figure 39. Initial conditions: dot-dash line 1000,1; dotted line 1000,2; solid line 2000,1; dashed line 2000,2.

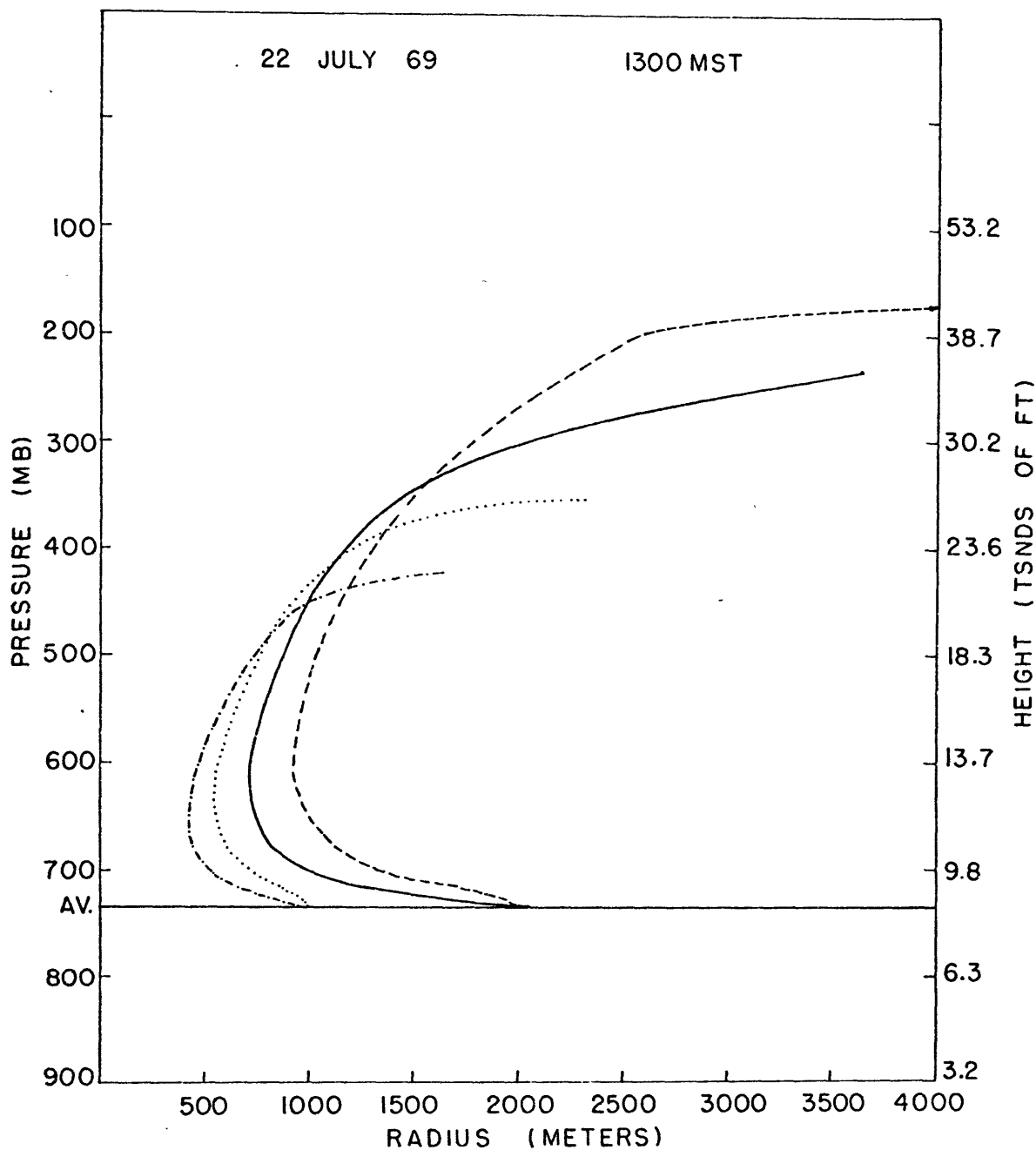


Figure 40. Initial conditions: dot-dash line 1000,1; dotted line 1000,2; solid line 2000,1; dashed line 2000,2.

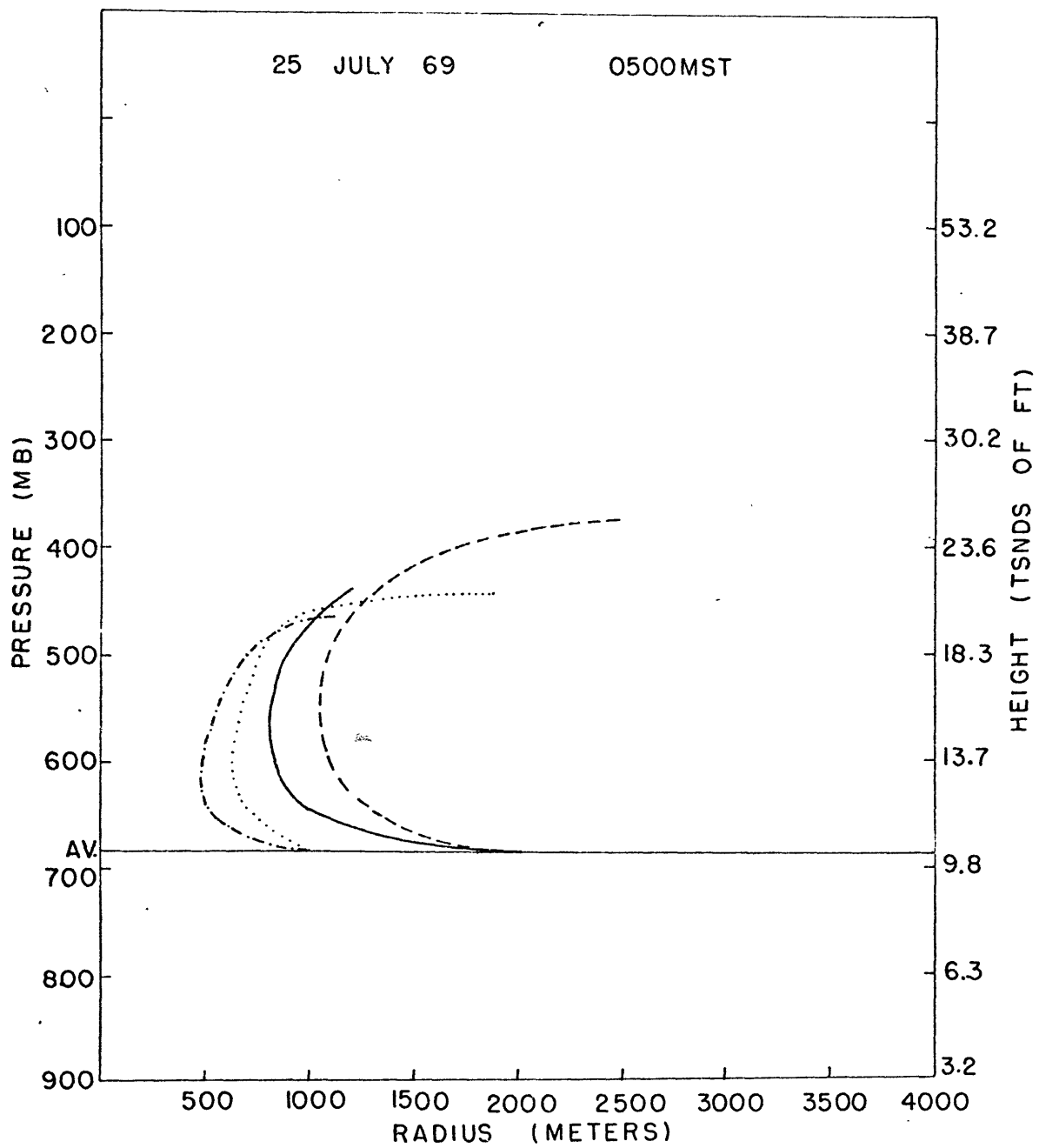


Figure 41. Initial conditions: dot-dash line 1000,1; dotted line 1000,2; solid line 2000,1; dashed line 2000,2.

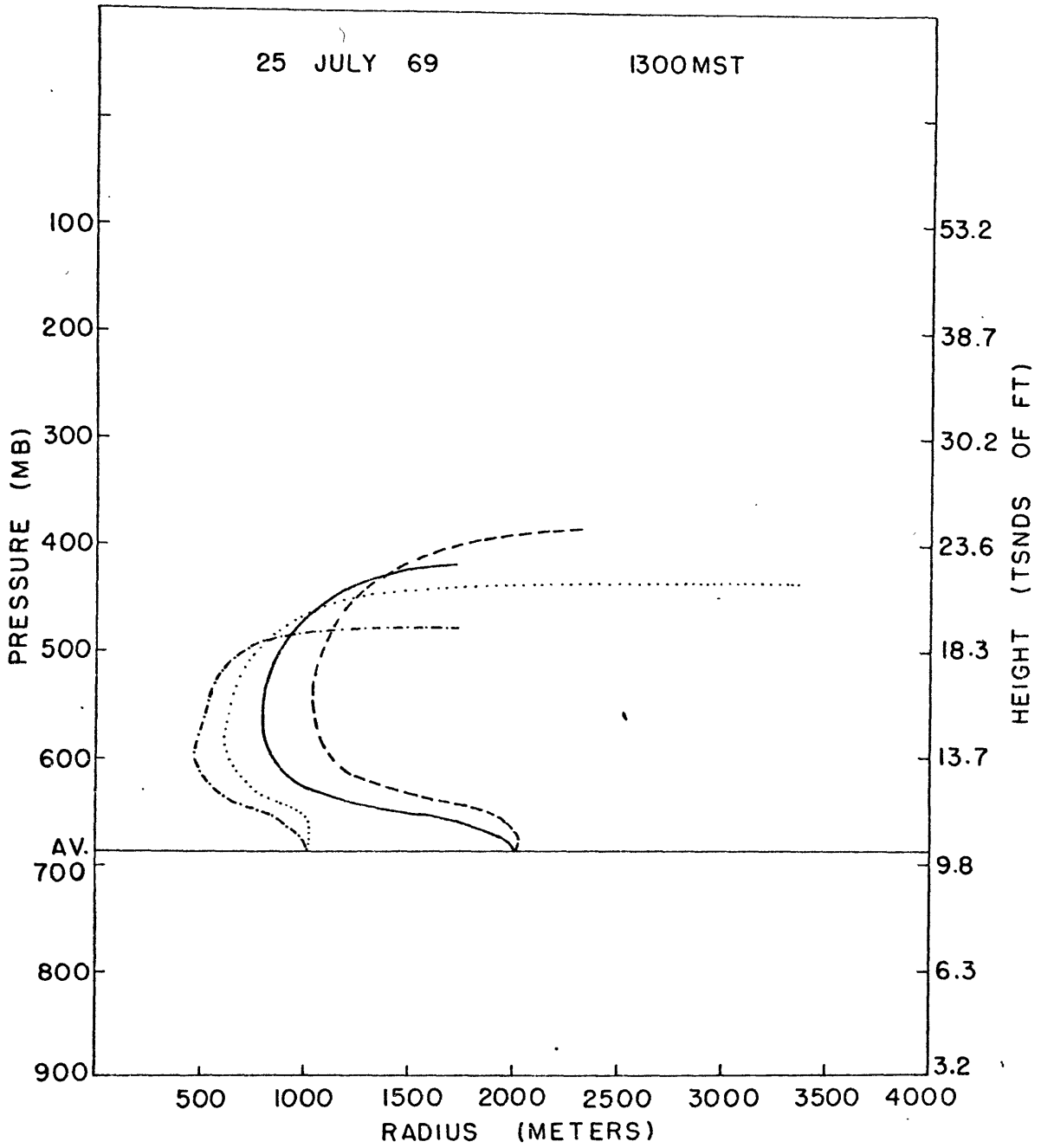


Figure 42. Initial conditions: dot-dash line 1000,1; dotted line 1000,2; solid line 2000,1; dashed line 2000,2.

Acknowledgments

I thank my advisor, Professor Edward Lorenz, for suggesting the area of research which led me to this thesis and for his support and guidance. I thank Professors Frederick Sanders and Norman Phillips for their helpful suggestions. Dr. Robert Cunningham and Dr. Morton Glass of AFCRL gave freely of their time, in assembling data and teaching me photogrammetric techniques. Miss Isabelle Cole drafted the lettering on the figures. Finally, I wish to thank my parents, Mr. and Mrs. E. Edward Buder, for their lifelong support and encouragement. This research was supported in part by the National Science Foundation under Grant No. GA-36107.

References

Brown, Henry A. and Morton Glass, 1970: "The use of a cumulus model in a cloud modification experiment," Second National Conference on Weather Modification, Santa Barbara, Cal., pp. 8-13.

"Cloud Puff IV Operations Plan," Earth and Planetary Sciences Division, Naval Weapons Center, Cloud Physics Branch, Air Force Cambridge Research Laboratories and Atmospheric Physics Division, White Sands Missile Range, Weather Science, Inc., Norman, Oklahoma, 1969, 32 pp.

Cunningham, Robert M., 1970: "Problems in evaluating effects of seeding cumulus clouds," Second National Conference on Weather Modification, Santa Barbara, Cal., pp. 193-197.

Glass, M., and T.N. Carlson, 1963: "The growth characteristics of small cumulus clouds," Journal of the Atmospheric Sciences, 20, pp. 397-406.

Gray, W., and R. Lopez, 1972: "Cumulus convection and larger scale circulations, Part I," Atmospheric Science Paper No. 188, Dept. of Atmospheric Sciences, Colorado State University, Fort Collins, Colo. 100 pp.

Greenough, Carol J., 1965: "Techniques of data reduction for ground based stereo photographs and aircraft recorded atmospheric variables," Final Report for Contract No. AF 19(604)-6616, prepared for AFCRL, Bedford, Mass., 66 pp.

Malkus, J., and G. Witt, 1959: "The evolution of a convective element. A numerical calculation," The Atmosphere and the Sea in Motion, Rockefeller Institute, Oxford University Press, pp. 425-439.

"Mesometeorological Field Studies," Final Report under Contract No. AF 19(604)-7259, prepared for AFCRL, Satellite and Mesometeorology Research Project, Dept. of the Geophysical Sciences, University of Chicago, 1965, pp. 23-26.

Morton, J., G. Taylor and J. Turner, 1956: "Turbulent gravitational convection from maintained and instantaneous sources," Proceedings of the Royal Society (A), 234, pp. 1-23.

Murray, F.W., 1970: "Numerical models of a tropical cumulus cloud with bilateral and axial symmetry," Monthly Weather Review, 98, pp. 14-28.

Scorer, R.S., and C. Ronne, 1956: "Experiment with convection bubbles," Weather, 11, pp. 151-154.

Silverman, Bernard A., 1959: "The effect of a mountain on convection," Proceedings of the First Conference on Cumulus Convection, Portsmouth, New Hampshire, pp. 4-27.

Simpson J., and A.S. Dennis, 1972: "Cumulus clouds and their modification," NOAA Technical Memorandum ERL OD-14, U.S. Dept. of Commerce Publication, 148 pp.

Squires P., and J.S. Turner, 1962: "An entraining jet model for cumulo-nimbus updraughts," Tellus, 14, pp. 422-434.

Weinstein, A.I., 1970: "A numerical model of cumulus dynamics and microphysics," Journal of the Atmospheric Sciences, 27, pp. 246-255.

Wiggert, V., 1972: "Cumulus simulations by a modified axisymmetric model, with comparisons to four observed tropical clouds," NOAA Technical Memorandum ERL OD-12, U.S. Dept. of Commerce Publication, 96 pp.